Catalytic Screening for the Production of Jet Fuel from Palmitic Acid

Auteur : Aregawi, Mearg Alem
Promoteur(s) : Richel, Aurore
Faculté : Gembloux Agro-Bio Tech (GxABT)
Diplôme : Master : bioingénieur en chimie et bioindustries, à finalité
Année académique : 2021-2022
URI/URL : http://hdl.handle.net/2268.2/15139

European Master in Biological and Chemical Engineering for a Sustainable Bioeconomy

Master thesis report

Submitted to obtain the degrees of

Master in Biology AgroSciences (BAS) of the University of Reims Champagne-Ardenne

Master of Science in Engineering of Tallinn University of Technology

Master in Bioengineering: Chemistry and Bioindustries of the University of Liège

Title of the Master thesis:

Catalytic screening for the production of jet fuel from palmitic acid

Presented by: ***AREGAWI Mearg Alem***

Date of the defense (dd/mm/yy): 21 /06 /2022

Supervised by:

Prof. Aurore Richel

Prof. Jaan Kers

Mr. Sergio Martínez

At: Gembloux Agro-Bio Tech-University of Liège

(Pass. des Déportés 2, 5030 Gembloux)

From: 24 /01 /2022 to 20 /06/2022

Confidentiality: No Privacy expiration date: …/…/….

[This page is intentionally left blank]

Copy right

Statement of responsibility

This document engages only its author.

Contents

List of Figures

Abstract

The growing concern over the depletion of fossil fuel and environmental pollution due mostly from the transportation sector has forced the search for alternative renewable fuels. Pyrolysis is a promising approach to convert lipids into fuels using catalysts. In the present work, pyrolytic deoxygenation of palmitic acid to jet fuel was studied without external supply of hydrogen to compare the performance of three catalysts, namely Pt/C, Ni/SiAl, and $CoMo/Al_2O_3$. The reaction products were analyzed by FTIR to verify the presence of unconverted fatty acid. The FTIR results which show a peak characteristic to C=O stretching at around 1708 cm^{-1} were subjected to fatty acid determination using GC-FID to validate the presence of unconverted palmitic acid and explore the presence of smaller carbon chain fatty acids. Products were also analyzed using GC-FID with HP-5 column to confirm the presence of hydrocarbons. The results reveal that Ni/SiAl results in higher cracking activity than $CoMo/Al_2O_3$ while Pt/C shows the highest performance giving complete conversion of palmitic acid at 2 hours and 270 ^{0}C of reaction time and temperature, respectively. Pentadecane was the main hydrocarbon produced by Pt/C. The study on the effect of reaction time, catalyst loading, and presence of water on conversion were also covered. The analytical instruments used did not allow for a complete identification of the product composition, hence no detail analysis of the yield and selectivity was performed.

Keywords: *jet fuel, deoxygenation, pyrolysis, hydrocarbon, pentadecane*

Acronyms

HDO	Hydrodeoxygenation
DCO	Decarbonylation
DCO2	Decarboxylation
BF_3	Boron fluoride
DCM	Dichloromethane
SiAl	Silica alumina
FAME	Fatty acid methyl ester

Introduction

Jet fuel is a blend of C_8-C_{16} hydrocarbons which is mainly composed of linear and branched alkanes (paraffins), aromatics, and cycloalkanes (naphthenes)(Fu et al. 2015). Paraffins, which have better burning properties (Bernabei et al. 2003), and cycloparaffins help reduce the freezing point of the fuel which is important when flying at high altitudes (Faroon, O.M., Mandell, D.M., & Navarro 1995). Aromatics are also important constituents of jet fuel used to keep the swelling of fuel system elastomers and the fuel's energy output per unit mass (Tian et al. 2016); however, the amount of aromatics in the jet fuel should be kept within an acceptable limit to avoid affecting the cleanliness of the fuel (Hileman and Stratton 2014; G. Liu, Yan, and Chen 2013).

The composition of conventional jet fuel varies depending on the original crude oil, but it typically contains 20% paraffins, 40% isoparaffins, 20% naphthenes, and 20% aromatics (Blakey, Rye, and Wilson 2011). The relative quantities of these hydrocarbon components are adjusted to meet the fuel's desired bulk properties, such as energy content, combustion characteristics, density, and fluidity (Dayton and Foust 2020). Owing to the difference in the proportion of these hydrocarbons, there are various types of Jet fuel. They are broadly classified into commercial and military jet fuels. Commercial jet fuel includes, Jet A, Jet A-1, and Jet B whereas military jet fuel comprises JP-4 and JP-8 (Atsonios et al. 2015). Jet B has a freezing point of -50 ^{0}C and resembles JP-4, while Jet A-1 has a freezing point of -47 ^{0}C and is similar to that of JP-8 (Goh et al. 2022).

The aviation sector is among the main contributors of greenhouse gas emissions. Every year, the aviation industry consumes about 2,000 million barrels of petroleum and is responsible for a significant portion of greenhouse gas emissions emitted into the environment (Díaz-Pérez and Serrano-Ruiz 2020). If no action is done or advances in engine technologies and flight operations are achieved, aviation CO_2 emission is anticipated to grow by three to seven times in 2050 compared to 2005 levels (Martinez-Hernandez et al. 2019). Thus, using renewable and sustainable aviation fuel (bio-jet fuel) to reduce carbon emissions and overall environmental effect is indispensable.

Nowadays, bio-jet fuel has gained acceptance in the aviation sector as one way of reducing greenhouse gases emission which is recognized by the International Air Transport Association (IATA)(Lim et al. 2021). Concerning CO_2 emissions, one of the aviation sector's goal is to reduce by 50 % in 2050 as compared to 2005 level (Ahmadi et al. 2015). Plants and algae are the only

carbon-containing renewable energy sources that are widely available and can directly absorb CO_2 from the air to generate organic matter (Wei et al. 2019) which can be further deployed for bio-jet fuel production. In other words, the carbon dioxide that was emitted by burning bio-jet fuel will be taken into plants and algae from the atmosphere by photosynthesis, resulting in carbon neutrality. In addition to low CO_2 emissions, bio-jet fuels provide the advantages of low tailpipe emissions, low sulfur content, high thermal stability, and strong cold flow qualities (Lokesh et al. 2015; Timko et al. 2011).

Lipids which are a group of organic compounds, including fats and oils, are easier to convert into liquid hydrocarbons than cellulosic biomass because they are already high-energy liquids with less oxygen (J. Xu, Jiang, and Zhao 2016). For that reason, vegetable oils are the most extensively utilized bio-jet fuel feedstock, but waste cooking oils, animal oils, and microalgae lipids are all promising (Tian et al. 2016). Palmitic acid (Figure 1) is one of the most abundant fatty acids found in the lipids of all organisms (William W. Christie 2012) and is regarded as a model compound. Therefore, deoxygenation of palmitic acid has been studied by many researchers under different reaction conditions (Jang et al. 2010; Lestari et al. 2009; Miao et al. 2016; Peng et al. 2013; Simakova et al. 2009).

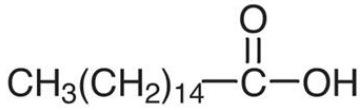

Figure 1: Palmitic Acid

Various methods are applied to convert different feedstocks into bio-jet fuel. Under ASTM D7566, there are four ASTM-certified bio-jet fuel production routes., namely Fischer-Tropsch synthesis (**FTS**), Hydroprocessed ester and fatty acid (**HEFA**), Alcohol-to-Jet synthetic paraffin kerosene (**ATJ**), Direct sugar to hydrocarbons (DSHC). Each of them has its own set of benefits and drawbacks(Xuebing Zhao et al. 2019).

Unrefined lipids can cause coking of the injectors, carbon deposits, oil ring sticking, and thickening of lubricating oils (J. Xu, Jiang, and Zhao 2016). Therefore, the removal of oxygen from fatty acids is vital to improve the quality of the fuel (e.g., increasing its higher heating value) to comply with internationally accepted jet fuel standards and replace the traditional petroleum-derived aviation fuels. Some of the above-mentioned techniques have drawbacks. For example, Fischer-Tropsch fuel has low energy density and low aromatic content which causes leakage

problems in the engine due to shrinkage of the engine (Hemighaus et al. 2006). HEFA bio-jet fuel involves the use of large amount of high pressure hydrogen (300–420 m^3 of H_2/ m^3 of vegetable oil) (Kubička 2008) supplied from petrochemical industry. Hence, the use of large amount of high-pressure hydrogen increases the overall cost of the process and contradicts with the goal of carbon emission. As a result, the search for other alternative technologies that do not rely on hydrogen is gaining attention.

Catalytic and non-catalytic (thermal) pyrolysis does not require hydrogen and can effectively convert lipids and fatty acids into hydrocarbons (Chiaramonti et al. 2016). When performed, is removed through a combination of hydrodeoxygenation (HDO), decarboxylation (DCO_2), and decarbonylation (DCO) reactions. HDO of fatty acids produces H_2O as a byproduct and paraffinic hydrocarbon having the same carbon number as original the fatty acid. On the other hand, decarboxylation (DCO_2) of fatty acids produces paraffinic hydrocarbons with the carboxyl group removed as CO_2 whereas decarbonylation (DCO) produces paraffinic hydrocarbons with carboxyl group removed as CO and H_2O (Edeh, Overton, and Bowra 2021). The consequent hydrocarbon from DCO and DCO_2 has one carbon less as compared to the original fatty acid, and in the case of DCO, an alkene is often produced.

Both catalytic and noncatalytic pyrolysis can produce a liquid product containing alkanes, olefins, aldehydes, ketones, and carboxylic acids; however, noncatalytic pyrolysis produces liquids with a high acid number due to low deoxygenation efficiency (J. Xu, Jiang, and Zhao 2016). Therefore, the use of catalysts is necessary to enhance the degree of deoxygenation and to improve the overall properties of the fuel, including burning properties.

Catalyst

Different catalysts with metal and acid sites are used for the deoxygenation process. These include metal sulfides (e.g., sulfided CoMoS and NiMoS), noble metal catalysts (e.g., Pt, Ru, Pd), and non-noble metal catalysts (e.g., Ni, Co, Fe). Among the heterogenous catalysts, metal sulfide catalysts are less expensive and show high activity in deoxygenation of triglycerides and model compounds, however, sulfur leaching leads to catalyst deactivation and sulfur contamination in liquid products (Soni et al. 2017). In addition, the sulfidation process occurs at high temperature and requires sulfiding agent to avoid catalyst deactivation (Satyarthi et al. 2013). On the other hand, non-sulfided noble metal catalysts have high reactivity at mild temperatures, require less or

no H_2, and do not contribute any sulfur contamination (Murata et al. 2010). Therefore, this study was done with noble metal catalysts and non-sulfided transition metal catalysts.

According to a study by Jelle Wildschut et al., ruthenium supported on activated carbon (Ru/C) has a high hydrodeoxygenation (HDO) activity, resulting in a deoxygenation level of 90% at 4 hours of residence time from a fast pyrolysis oil (Wildschut et al. 2009). Ruthenium has also resistance to deactivation in the presence of water (Goh et al. 2022). Ruthenium, however, has lesser catalytic activity than Pd and Pt (Galadima and Muraza 2015a), and its large scale applicability is limited by its high cost and poor reusability (Hansen, Mirkouei, and Diaz 2020).

It is of critical scientific interest to use supported transition metal catalysts, such as nickel and cobalt, with intermediate acid–base characteristics for selective conversion of lipids into hydrocarbon fuels due to their low cost and promising performance in hydrogenation and hydrogenolysis reactions. Nickel can replace the most expensive noble metals since it exhibits properties similar to noble metals (De et al. 2016). Many studies reported that both nickel and cobalt exhibited high activity for the deoxygenation of lipids into hydrocarbons. A 100% conversion of palmitic acid was achieved using nickel based catalyst at 260 ^{0}C, 12 bar H_2, and 6 h residence time (Peng et al. 2013). A. Srifa et al. obtained 88.5% and 67.7% liquid product yield composed of n-alkanes, oxygenated intermediates, alcohols, esters, and fatty acids from refined palm oil using 5% Co/Al_2O_3 and 5% Ni/Al_2O_3, respectively (Srifa et al. 2015). When the catalyst loading was reduced, however, the yield lowered. This clearly shows how the catalyst loading affects yield. Ni/SiAl has been found to be a promising catalyst for the deoxygenation of triglyceride-based feedstock due to its low cost and no need for sulfidation (Venter, Schabort, and Marx 2015).

Usually, nickel and cobalt are used in a bimetallic catalytic system where they combine with other metals, such as molybdenum (Mo), copper (Cu), iron (Fe), and tungsten (W) to improve their hydrodeoxygenation efficiency (Goh et al. 2022). A. Rafiani et al. have noticed that the yield of octadecane increased after iron (Fe), copper (Cu), and cobalt (Co) metals were added to Ni/SiAl (Rafiani et al. 2020). $NiMo/Al_2O_3$ has shown good catalytic activity in the production of alkanes with limited degree of side reactions (Galadima and Muraza 2015b). Hydrodeoxygenation degree of 99.6% and 99.3% were obtained from waste cooking oil using $NiMo/Al_2O_3$ and $CoMo/Al_2O_3$, respectively (Toba et al. 2011). N. Asikin-Mijan et al. reported that $NiO\text{-}CaO_5/SiAl$ produced 73% of hydrocarbon yield and the catalyst can be reused up to four times without significant loss in its

catalytic activity (Asikin-Mijan et al. 2017). Nevertheless, nickel and cobalt are less selective to decarboxylation reaction (Madsen et al. 2011) and less active than platinum under hydrothermal conditions (Duan et al. 2013; Madsen et al. 2011). Furthermore, high interaction of large cobalt particles with fatty acids could result in adsorption of fatty acids on the active sites leading to the deactivation of the catalyst (Phichitsurathaworn et al. 2020). The activity of nickel is also dependent on the method of catalyst preparation used (De et al. 2016).

Both palladium (Pd) and Platinum (Pt) are the most active catalysts for deoxygenation of fatty acids. It has been reported that Pd and Pt have been used for large scale production of hydrocarbon fuel (Khan et al. 2019a). Unlike Ru which favors the catalysis of HDO reaction, Pd and Pt have excellent catalytic activity for DCO and DCO_2 reactions. According to some studies, DCO and DCO_2 routes are theoretically more economical than HDO route (Srifa et al. 2015). High oxygen removal can be found with Pd/γ-Al_2O_3 than Pt/γ-Al_2O_3 and Ni/γ-Al_2O_3, however, Pd/γ-Al_2O_3 was found to be only slightly more active than Pt/γ-Al_2O_3 (Madsen et al. 2011). Over 90% selectivity was achieved with 5% Pt/C from palmitic acid (Fu, Lu, and Savage 2011). Srifa et al. have studied the effects of various metals, such as platinum (Pt), palladium (Pd), nickel (Ni), and cobalt (Co) supported on γ-Al_2O_3 and they obtained that Co was responsible for HDO, DCO, and DCO_2 whereas platinum (Pt), palladium (Pd), and nickel (Ni) promoted DCO and DCO_2 of palm oil (Srifa et al. 2015). However, the highest selectivity was obtained using Pt/γ-Al_2O_3 or Pt/SAPO-11.

Furthermore, Jie Fu et al. have shown that 5% Pd/C and 5% Pt/C are very effective for hydrothermal deoxygenation with no H_2 added and show high selectivity towards pentadecane (Jang et al. 2010). The researchers also demonstrated the reusability potential of both catalysts with no significant loss in the catalytic activity. In another study by Jie Fu et al., aviation fuel was synthesized directly from microalgal lipids using Pt/C catalyst without addition of H_2 and demonstrated the reusability of the catalyst even after third use (Fu et al. 2015). Different studies also show that Pd and Pt catalysts supported on activated carbon are active for deoxygenation of fatty acids and have selectivity for the corresponding alkane (Jang et al. 2010; Lestari et al. 2009; Simakova et al. 2009; Snåre et al. 2006b). Therefore, Pt/C support seems the most promising catalyst.

Although both Pt and Pd show very good catalytic activity towards DCO and DCO_2, the subsequent isomerization is important to produce bio-jet fuels. In this regard, Pt has been known

to exhibit excellent catalytic activity and selectivity of n-alkanes isomerization (Goh et al. 2022). Pt with minimal acidity, optimum value of dispersion, and high electron density can give high level of conversion rate and hydrodeoxygenation selectivity (Janampelli and Darbha 2021). However, different supports could have varying acidity which could affect the dispersion of Pt for the hydrodeoxygenation reactions (Goh et al. 2022). Therefore, the selection of appropriate support is important.

Different supports have been used in the heterogeneous catalytic system for the HDO reactions. These include metal oxides (TiO_2, Al_2O_3, SiO_2, CeO_2, ZrO_2) (Bagheri, Muhd Julkapli, and Bee Abd Hamid 2014), zeolites (ZSM-5, HY, H-Beta) (Galadima and Muraza 2015b; T. Li et al. 2015; Xianhui Zhao et al. 2017), mesoporous material (MCM-41, SAPO-11, SBA-15, Al-SBA-15, Al-MCM-41) (Galadima and Muraza 2015b) and activated carbon (AC) (de Sousa, Cardoso, and Pasa 2016).

Carbon materials have a dual role as a catalyst and/or a catalyst carrier in many industrially essential reactions due to their good electron conductivity, structural flaws, high porosity, large specific surface area, high thermal stability, and chemical inertness over a wide pH range (Konwar and Mikkola 2022). Indeed, activated carbon has been considered to be one of the most promising catalytic supports (Oubagaranadin and Murthy 2011).

Many varieties of zeolites have been developed and used as a support for metal catalysts. There are about 200 varieties of zeolites and only a few have been used in large-scale (T. Li et al. 2015). Zeolites have high cracking activity, remarkable selectivity to bio-jet fuel, and strong resistance to deactivation (D. Li et al. 2015). However, conventional zeolites do not have pore sizes larger than 1.3 nm, which are not suitable for large molecules such as bio-oils (Cheng et al. 2019). This could limit the use of the support for large-scale applications. Moreover, zeolites have acidic nature which results in high coke formation (Xianhui Zhao et al. 2017).

TiO_2 have been used to modify catalysts to enhance their reusability. Chuhua Jia et al., have reported that Ru/C catalysts modified by TiO_2 showed good stability after five consecutive reuse cycles whereas unmodified Ru/C catalyst cannot fully restore its catalytic activity even after washing and reactivation (Jia et al. 2021). The modified catalyst also increased deoxygenation rate up to five folds. Nevertheless, the use of TiO_2 as a support will increase the overall cost of the catalyst. The catalyst preparation is also energy intensive and complex. Although Ru/γ-Al_2O_3 has higher dispersity, the oil yield and oxygen removal activity (at 200 ^{0}C, 100 bar, and 4 h) was lower

than Ru/TiO_2 and Ru/C due to its smaller specific surface area and relatively low stability (Wildschut et al. 2009). On the other hand, Ru/TiO_2 gives lower deoxygenation activity than Ru/C (Wildschut et al. 2009) which could be attributed to the lower surface area of TiO_2 (Elliott, Sealock, and Baker 1993; Osada et al. 2006).

Acid–base property of catalyst support plays the vital role in mediating catalytic activity and product selectivity. Generally, supports with moderate acidity are always preferred for bio-jet fuel production because high acidity can cause cracking of alkanes (Galadima and Muraza 2015b) while catalyst support with high basicity have high selectivity to heavy alkanes with high carbon number due to ketonization coupling of fatty acid intermediates (Snåre et al. 2006a).

Alumina has been the most widely used support due to its many attractive properties including high specific surface area, good physical strength, moderate acidity, and resistance to thermal degradation (Goh et al. 2022). Modification of the alumina support with silica was found to improve the deoxygenation activity of the NiMo catalysts (Mo et al. 2009). Silica alumina has also good mechanical and thermal stability (Rafiani et al. 2020). SAPO-11 has also moderate acidity and high selectivity to n-C_7-C_{14} alkanes (Galadima and Muraza 2015b). Many studies reported that moderate acidity promotes the isomerization of alkanes. According to M. Rabaev et al., Pt over SAPO-11 or Al_2O_3 support enhances the isomerization of saturated alkanes into branched alkanes, which improves the fuel's cold flow characteristic (Rabaev et al. 2015). Moreover, γ-Al_2O_3 supported catalyst can be easily regenerated by calcination after deactivation (T. Li et al. 2015). This improves the reusability of the catalyst. However, γ-Al_2O_3 reacts with acidic water at elevated conditions leading to reduction of its surface area (Wildschut et al. 2009).

Hence, to avoid deactivation of the supports and to optimize the performance of the given catalyst, the reaction conditions should be carefully chosen. The conversion, yield, and selectivity to bio-jet fuels depend on parameters, such as temperature, residence time, and production mode. The effect of each parameter is discussed as follows.

Production mode

Batch and semi-batch mode of production have been used in the deoxygenation of triglyceride based oils for the production of liquid hydrocarbons (Romero et al. 2016). Extended reactions (i.e., longer residence time) give high proportion of hydrocarbons in batch mode of production (Khan et al. 2019b). Romero et al. have demonstrated the effect of production mode on the yield of hydrocarbons. According to their research, a batch mode produced a single phase

containing 80% hydrocarbons, whereas a semi-batch mode produced a light fraction containing 72-80% hydrocarbons and an intermediate fraction containing 85-88% hydrocarbons (Romero et al. 2016).

Reaction temperature

Reaction temperature is among the key factors that affect the product distribution, yield, and selectivity of bio-jet fuel range alkanes. The effect of reaction time on the yield and selectivity of liquid hydrocarbons have been studied by many researchers. A study on the catalytic deoxygenation of oleic acid at different temperatures 240, 250, 260 ^{0}C reveals that the conversion increased from 88.9% to 100% as the reaction temperature increased from 240 to 250/260 ^{0}C owing to increased catalytic activity at increased reaction temperature(Feng, Niu, et al. 2020). This indicates that a small change in temperature cold result in a significant difference in conversion.

Least amount of coke formation and optimum C=O bond scission of fatty acids can be attained using catalysts at reaction temperature of 350-375 ^{0}C(Arun, Sharma, and Dalai 2015). However, further increase in temperatures can cause severe cracking and coke formation. Q. Liu et al. investigated the effect of temperature on deoxygenation of palm oil. The researchers observed that the liquid alkane yield (C15-C18 fraction) decreased with increase in temperature from 320 to 360 ^{0}C using Ni/SAPO-11(Q. Liu et al. 2014) which implies increased cracking caused by high temperature. Selectivity of hydrocarbons was found to increase from 44 to 79% with decrease in temperature from 320 to 280 ^{0}C (Galadima and Muraza 2015a). Therefore, relatively lower temperatures (i.e., temperatures around 280 ^{0}C) seem to be better not only to minimize severe cracking but also to reduce energy consumption of the process.

Reaction time

Reaction time is the length of time spent by the reaction mixture in the reactor. In continuous reactors, the term space velocity is frequently used (i.e., the number of reactor volumes of feed that can be processed in a unit time or flowrate of the feed divided by volume of the reactor). The higher space velocity the shorter residence time.

M. Anand et al. have reported that the conversion of triglycerides decreased with decreased residence time at all temperatures, 340-420 ^{0}C (Anand et al. 2016). A similar result was determined by V. Itthibenchapong et al. in which the yield of liquid hydrocarbons decreased as the liquid hourly space velocity increased from 1 hr^{-1} to 5 h^{-1}(Itthibenchapong et al. 2017). However, very short residence time could also result in a very low yield and selectivity. A study carried out by

Suwannasom et al. indicates that the very low selectivity (i.e., 24.8%) was obtained at 30 min residence time while the selectivity increased to 30.15% when the residence time was increased to 120 min (Khan et al. 2019b). Nevertheless, further increase in residence time decreased the yield and selectivity of jet fuel. As a result, before scaling up the process, the optimum residence time should be identified.

In this study the deoxygenation performance of different catalysts was compared based on degree of conversion and cracking of palmitic acid at relatively mild temperature without addition of external hydrogen. Owing to the limitation with the maximum operation temperature of the available reactor, all the reactions were undertaken at 270 ^{0}C unless mentioned. The study also explores the effect of reaction time, catalyst loading, and addition of water on conversion of palmitic acid.

Methodology

Solvents, reagents, and chemicals

The catalysts, namely 5wt% Pt/C, Ni/SiAl (65±5% Ni), and $CoMo/Al_2O_3$ (Cobalt oxide, typically3.4-4.5%, Molybdenum oxide typically 11.5-14.5%) were purchased from thermoscientific. Supelco 37 component fatty acid methyl ester (FAME) Mix, Dichloromethane (DCM), n-hexane (95% purity), chloroform, palmitic acid, sulfuric acid (95% purity), boron fluoride (BF_3), and methanol, were all analytical grade chemicals. All catalysts were used as received without prereduction. A multicomponent mixture of 19 hydrocarbons was purchased from Agilent technologies.

Catalyst selection

A thorough literature study was performed to select catalysts from noble metals, supported monometallic, and bimetallic catalysts. Various variables have been considered, including cost, reusability, availability, and catalytic activity based on yield, conversion, and selectivity reported in literature. When screening the catalysts, the reaction conditions stated in the literature were also taken into consideration to cope with the limitations on hand.

Deoxygenation experiment

Both thermal cracking (pyrolysis) and catalytic deoxygenation of palmitic acid in water were undertaken in a 50 mL batch parr reactor. Only Pt/C catalyst was used to study the catalytic deoxygenation of palmitic acid in water. A known amount of palmitic acid, 4:1 weight ratio water to palmitic acid (i.e., for reactions involving catalytic deoxygenation in water), and 16wt% of catalyst were added into the reactor. For Pt/C, different catalyst loadings have been studied. After adding palmitic acid, catalyst, and water (i.e., for reactions involving catalytic deoxygenation in water) into the reactor, the reactor was sealed and tightened. To remove air and produce an inert environment, the reactor was purged three times with nitrogen gas at 6.5 bars. Unless otherwise stated, all experimental runs were conducted at a temperature of 270°C. All reactions were performed in a nitrogen atmosphere at pressure of 6.5 bars. No gas phase quantification was undertaken.

After the reaction time has reached, the reaction was stopped and cooled to 70 ^{0}C. Then the reactors were put in cold water bath for 15 minutes to speedup cooling. The reactors were rinsed with 20-40 mL of dichloromethane and the mixture was filtered to separate the catalyst and solid

residue from the liquid products. The filtrate was stored in pre-weighed falcon tubes, which were left open in the fume hood for 24-72 hours to allow the dichloromethane to evaporate. Finally, the weight of the liquid or solid remaining in the falcon tube was measured to calculate the yield of liquid product. The yield was calculated as follows:

$$Liquid\ yield = \frac{weight\ after\ evaporating\ DCM - weight\ of\ falcon\ tube}{weight\ of\ palmitic\ acid\ loaded\ into\ reactor} \times 100$$

Product analysis

i. FTIR

Bruker Vertex 70 Attenuated total reflectance-Fourier transform infrared spectroscopy (ATR-FTIR) was performed using OPUS software to identify the chemical constituents, elucidate the compound structures, and compare the types of functional groups in the liquid and solid products of all samples. First, the ATR-FTIR machine was purged with N_2 to remove humidity until the humidity sensor turned green. 5µL of liquid products from Pt/C catalyzed pyrolytic reaction were directly injected for analysis whereas the solid products were solubilized in 5 mL of chloroform to homogenize the sample before injecting into the ATR-FTIR machine. Then, ~3µL of the solution was then taken and injected in the ATR-FTIR machine. The readings were taken from 400 to 4000 cm^{-1}.

In addition to analysis methods presented above, the density of liquid products from Pt/C catalyzed pyrolytic reactions (at reaction time 2h, 3h, and 4h, temperature of 270 ^{0}C, and 16wt% catalyst loading), were also determined to compare it with the density of standard jet fuel. To determine the density, 30 µL of each sample was weighed and the average ratio of the weight to volume was considered as the density of the liquid sample.

ii. Fatty acid determination

Gas chromatography with a flame ionization detector (GC-FID) and HP-INNOWAX column (30m × 0.250mm × 0.25µm) was used to verify the presence of unconverted palmitic acid and other fatty acids in all products of Ni/SiAl and $CoMo/Al_2O_3$ catalyzed pyrolytic reaction and from Pt/C catalyzed reaction that contain solid in the reaction products by derivatizing the fatty acids with methanol.

First, BF_3 reagent was prepared by mixing BF_3 solution (14wt% in methanol) with methanol and hexane in 25:55:20 v/v/v ratio. A known amount of hexane was added to the solid samples in such a way that the weight of the solid to the volume of hexane became 50:1 (mg/mL). After that,

0.2 mL of the sample and 0.5 mL of BF_3 reagent were added into a sovirel tube. The sovirel tubes were hermetically sealed to avoid hexane evaporation and placed in a water bath at 70°C for 1 hour and 30 minutes.

After the reaction time has reached, the sovirel tubes were removed from the water bath. Thereafter, 0.5 mL of saturated NaCl solution 0.2 mL and 10% H_2SO_4 solution were added and shaken using vortex mixer. Then, 7-8 mL of hexane was added and shaken vigorously using vortex mixer. Finally, 0.5 µL of the upper phase was taken and injected into GC-FID.

"Supelco 37 component FAME Mix" was used as a standard mixture of FAMEs that contains 37 known FAMEs. 0.5 µL of the standard mixture was injected for a GC analysis according to FAME3 method (6890_FAME_HP INNOWAX). The GC oven temperature was programmed as: a 1 min hold at 50 ^{0}C, 30 ^{0}C /min ramping to 150 ^{0}C, 4 ^{0}C /min ramping to 240 ^{0}C, 10 min hold at 240 ^{0}C. After determining the chromatogram of all samples, each peak in each chromatogram was assigned to the corresponding FAME by referring to the retention times in the standard and the supplier.

iii. Hydrocarbon analysis

The determination of fatty acids was carried out only to the products that contain solid phase from Pt/C, Ni/SiAl and $CoMo/Al_2O_3$ catalyzed pyrolytic reactions. However, the liquid products produced by Pt/C catalyzed pyrolytic reactions (at reaction time of 2h, 3h, and 4h, temperature of 270 ^{0}C, and 16wt% catalyst loading), were analyzed by gas chromatography with flame ionization detector (GC-FID) and HP-5 column (30m × 0.320mm × 0.25µm) to substantiate the presence of hydrocarbons in the liquid products. The GC oven temperature was programmed as follows: a 1 min hold at 35 ^{0}C, 10 ^{0}C/min ramping to 325 ^{0}C. The detector temperature was maintained at 325 ^{0}C. A multicomponent mixture of 19 hydrocarbons was used as a standard.

Results and Discussion

Catalyst screening

The table given in Appendix (Table 1) is the data gathered from literature to compare and screen various catalysts used in different studies based on their activity, cost, availability in market. In addition, the reaction conditions, such as the temperature, reaction time, the use of external hydrogen, catalyst loading, and recyclability were all considered to reach the final decision of the selection of catalyst. Owing to the absence of the necessary equipment to synthesize catalysts, only commercially available catalysts were considered. Moreover, the maximum operating temperature of the available parr reactor is 300 ^{0}C. Having these and other limitations, only three catalysts, namely Ni/SiAl, CoMo/Al_2O_3, and Pt/C were selected.

Results of deoxygenation experiment

Mass balance

The following figure (Figure 2) shows the comparison of mass balances between three similar reactions catalyzed by different catalysts (i.e., Pt/C, CoMo/Al_2O_3, and Ni/SiAl). Solid residue refers to the cumulative weight of catalyst, and coke or other unidentified components that remain in the filter paper after filtration. The weight that has disappeared (loss) is calculated as follows:

$$Loss\ (g) = Input(g) - solid\ residue(g) - product\ (g)$$

Various possible reasons could lead to the disappearance or loss of mass. Ideally, all the catalyst which was added to the reactor should be recovered in the filter paper after filtration. Unreacted palmitic acid should also be found in the product mixture. However, it is always possible to have some loss of mass due to sticking of the reaction mixture to the surface of the reactor, tubes, vacuum flask, and filtration funnel. The loss could also stem from the production of gases, such as CO_2 and CO because of DCO_2 or DCO, respectively. The production of volatile hydrocarbons, such as, propane, butane, pentane, hexane, etc. which evaporate after the product mixture were left open in the fume hood could also result in loss of weight.

From the figure below and (Figure 23 and Figure 24 in Appendix), it can be clearly seen that both Pt/C and Ni/SiAl catalyzed reactions display higher loss than CoMo/Al_2O_3 catalyzed reactions. This may be due to higher degree of cracking leading to release of CO_2 and CO suggesting higher activity of both catalysts as compared to CoMo/Al_2O_3 at all reaction times. In

addition, $CoMo/Al_2O_3$ catalyst were bigger in particle size whereas Pt/C and Ni/SiAl are fine powders. Therefore, it is more probable to have more losses in the case of Pt/C and Ni/SiAl due to sticking onto the surface of the reactor and reactor tubes. On the other hand, Agglomeration of catalyst with the reaction mixture was commonly observed in $CoMo/Al_2O_3$ catalyzed reactions, resulting in big solid particles. This could explain why $CoMo/ Al_2O_3$ catalyzed reactions have a lower loss and a higher amount of solid residue recovered.

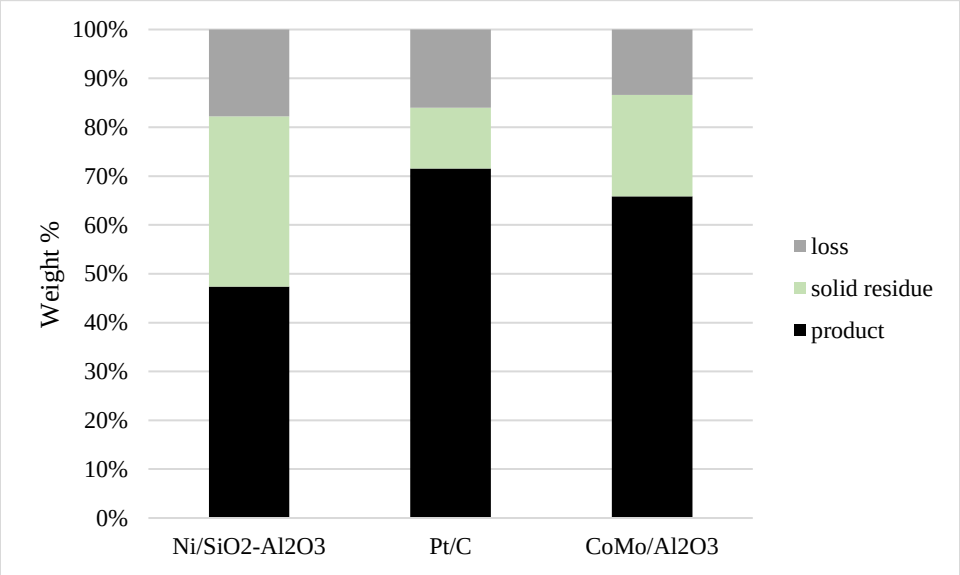

Figure 2: Comparison of mass balance between Pt/C, Ni/ SiAl and $CoMo/Al_2O_3$ catalyzed reactions (Temp= 270 ^{0}C and Time=3h)

Liquid yield and density

No liquid products were obtained from Ni/ SiAl and $CoMo/Al_2O_3$ Catalyzed reactions regardless of the change in reaction time. On the other hand, Pt/C at reaction temperature of 270 ^{0}C and 16wt% catalyst loading produced 71.57wt%, 65.37wt%, and 68.33wt% of liquid products at 2, 3, and 4 hours of reaction time, respectively. The result of the density of the liquid products was found to be 770.00 kg/m^3, 791.67 kg/m^3, and 813.33 kg/m^3 from the reaction times 2h, 3h, and 4h, respectively.

Product analysis

i. FTIR

Figure 3 shows the FTIR spectra of the liquid products from Pt/C catalyzed reaction (red spectrum), solid products from Ni/ SiAl (blue spectrum) and $CoMo/Al_2O_3$ (light green spectrum) catalyzed reactions (at 270 ^{0}C, 16wt% catalyst loading, and 2 hours). The spectra of products of

both Ni/SiAl and CoMo/Al_2O_3 catalyzed reaction are nearly identical. This indicates that the overall composition of the products are similar (Han et al. 2019). Both products show prominent absorption band at 1,708.48 cm^{-1} which is attributed to C=O stretching present in the carboxylic acid (Salimon, Salih, and Abdullah 2011). This implies that the conversion of palmitic acid to hydrocarbons wasn't complete and hence both catalysts have lower deoxygenation activity at the studied reaction conditions than Pt/C. On the other hand, the peak at 1708 cm^{-1} is completely absent in the liquid products of Pt/C catalyzed reaction which proves the absence of C=O functional group, hence 100% conversion of palmitic acid. H. Nam et al. reported the decrease in the absorbance peak height of the upgraded algal bio-oil due to the deoxygenated chemicals in the upgraded product (Nam et al. 2017). Similar result was also reported by R. Shakya et al. where the absorption peak at 16901730 cm^{-1} was completely absent after upgrading algal biocrude as a result of decarboxylation (Shakya et al. 2018). The peaks at 1,214.61 cm^{-1} for the Ni/ SiAl (blue spectrum) and CoMo/Al_2O_3 (light green spectrum) catalyzed reaction products are due to C-H bending (Nishida et al. 2012).

The bands appearing in the range of 2,850-2,975 cm^{-1} are due to symmetric and asymmetric stretching of C-H bonds in -CH_3 and -CH_2 of aliphatic compounds present in the solid product of Ni/SiAl, CoMo/Al_2O_3, and liquid products of Pt/C catalyzed reactions (Shakya et al. 2018). The liquid products of Pt/C catalyzed reaction (red spectrum) manifests a higher intensity of these bands which indicates the main presence of many C-H bonds (El-Lateef 2013). The smaller peaks at 1370-1380 cm^{-1} are assigned to CH_3 bending (Votano, Parham, and Hall 2004). The liquid products of Pt/C catalyzed reaction show an intense band at 1465 cm^{-1} which is characteristic to the deforming vibrations corresponding to C–H groups of alkane (Nosal et al. 2021).

The FTIR spectra in Appendix (Figures 10 and 11) are similar to those in Figure 4, indicating that functional groups are similar regardless of the reaction time. Hence, 4 hours of reaction time is still not enough to achieve complete conversion of palmitic acid by Ni/ SiAl and CoMo/Al_2O_3 catalysts. Conversely, Pt/C can give 100% conversion at 2 hours of reaction time.

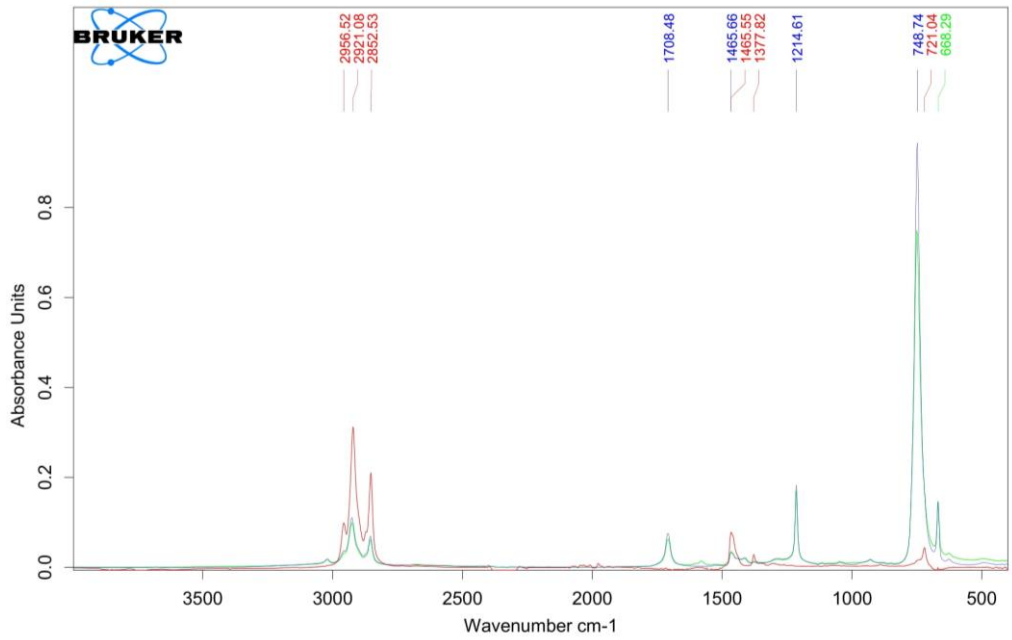

Figure 3: FTIR of Pt/C catalyzed (red), Ni/ SiAl catalyzed (blue) and CoMo/Al_2O_3 catalyzed (light green) products. (Reaction time= 2h, temperature= 270 ^{0}C, catalyst loading=16wt%)

Figure 4 below shows the FTIR spectra of products of Pt/C catalyzed pyrolytic reaction products at 270 ^{0}C and 1h, 2h, 3h, and 4h residence time. The three spectra of the products from 2h, 3h, and 3h reaction time are identical and undistinguishable from each other. This implies that the reaction times above 2h have no influence on the composition of the product. This can also be verified from Figure 12 and Figure 13 (Appendix) which show similar comparison of FTIR spectra of Ni/ SiAl catalyzed and CoMo/Al_2O_3 catalyzed reaction products, respectively.

Pt/C gives incomplete conversion when the reaction time is reduced to 1h. As can be seen in Figure 3 a small peak appears at 1708 cm^{-1} which is characteristic to C=O bond stretching present in unconverted fatty acids. In addition, lower intensity of absorption peak is observed at bands appearing in the range of 2,850-2,975 cm^{-1} which are due to symmetric and asymmetric stretching of C-H bonds in -CH_3 and -CH_2 of aliphatic compounds. Therefore, increasing the reaction time from 1h to 2h results in complete deoxygenation of palmitic acid and higher symmetric and asymmetric stretching of C-H bonds.

When the reaction takes place in the presence of water, however, all the spectra show the peak at 1708 cm^{-1} (Figure 14) and have lower intensity of absorbances as compared to the spectra of products from pyrolysis. Therefore, the presence of water affects the catalytic activity at the studied reaction conditions, hence reduced conversion of palmitic acid. The low conversion of

palmitic acid in the presence of water occurs as a consequence of stabilization of fatty acids under subcritical water (Watanabe, Iida, and Inomata 2006). In addition, The FTIR spectra are nearly identical at all reaction times (i.e., 1h, 2h, and 3h).

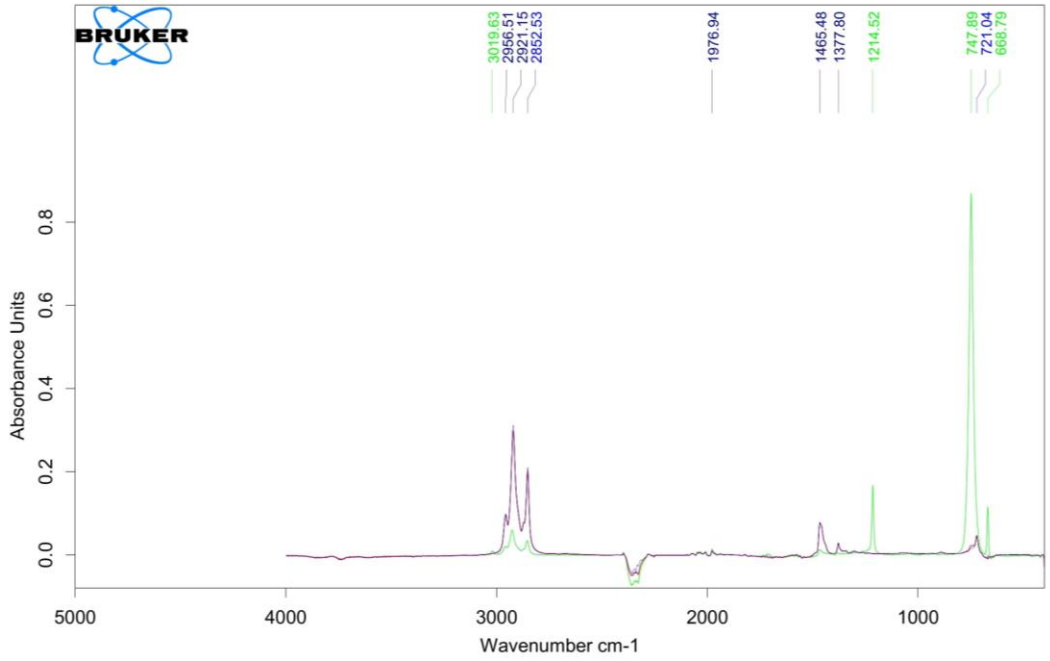

Figure 4: FTIR spectra of Pt/C catalyzed pyrolytic product from catalytic at 270 ^{0}C and different residence time (light green=1h, blue=2h, red=3h, and dark blue=4h).

The following figure (Figure 1Figure 5) and (Figure 16 and Figure 17 in Appendix.) show the comparison of FTIR spectra of products of pyrolysis versus reaction in water at 2h, 3h, and 1 of reaction time, respectively. The reaction temperature and Pt/C loading are 270 ^{0}C and 16wt%, respectively. Except for the addition of water in the second reaction, all other reaction conditions were the same. From all the figures it can be observed the presence of C=O stretching (peak at 1708 cm^{-1}) present in the unconverted carboxylic acid when the reaction was undertaken in the presence water which implies that water leads to low conversion of palmitic acid into hydrocarbons at the studied reaction conditions. This also indicates that the extended reaction time from 1h to 3h is not enough to achieve 100% conversion of palmitic acid when the reaction is carried out in water.

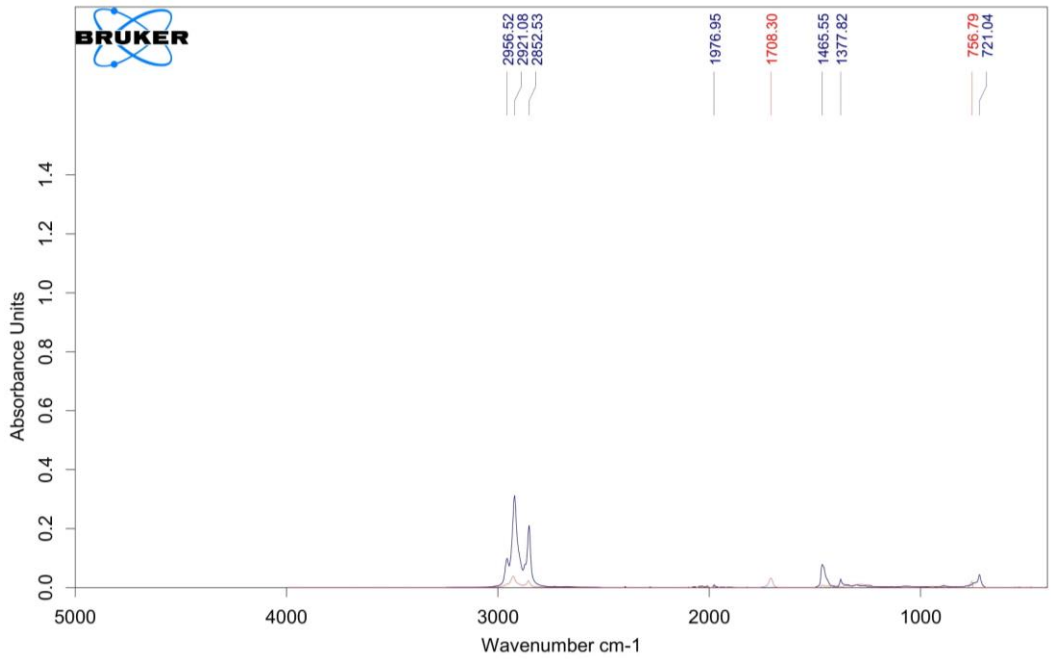

Figure 5: FTIR spectra of Pt/C catalyzed reaction product from catalytic pyrolysis and reaction in water at 270 ^{0}C and 2h (Red= reaction in water and Blue= pyrolysis)

Furthermore, ATR-FTIR analysis was carried out to compare the effect of Pt/C loading on the chemical composition of the product. As given in Figure 15 (Appendix), 8wt% loading gives lower conversion of palmitic acid as there is a peak characteristic to C=O at 1708 cm^{-1} due to the presence of unconverted palmitic acid or smaller carbon fatty acids. On the other hand, the peak characteristic to carboxylic acid is completely missing or is very small when the catalyst loading increased to 12wt% and 16wt%. In addition, the absorption intensity at 2,850-2,975 cm^{-1} which are caused by the symmetric and asymmetric stretching of C-H bonds in $-CH_3$ and $-CH_2$ of aliphatic compounds also increased in order of catalyst loading. This clearly demonstrates the effect of catalyst loading on conversion. Hence, Pt/C loading in the range between 12wt%-16wt% could give high conversion of palmitic acid into products in 2 hours of reaction time in the absence of water.

ii. Fatty acid determination

All products that have shown a peak characteristic to C=O stretching of fatty in the FTIR analysis were subjected to fatty acid determination to validate the presence of unconverted palmitic acid and other short carbon chain fatty acids produced as a result of cracking of palmitic acid. Figure 6 *a* and *b* show the GC-FID chromatograms of the products of Ni/SiAl and $CoMo/Al_2O_3$ catalyzed pyrolytic reactions, respectively. Except for catalyst type, both reactions have the same

reaction conditions (i.e., temperature of 270 ^{0}C, 16wt% catalyst loading, and 3 hours of reaction time). The peak at ~11.65 min is assigned to methyl palmitate; hence, it is noticeable from the chromatograms that both Ni/SiAl and CoMo/Al_2O_3 catalysts give incomplete conversion of palmitic acid.

By referring to the figure, Ni/SiAl gives higher conversion of palmitic acid than CoMo/Al_2O_3 in which methyl palmitate accounts for 60.80% and 87.40% of total peak area, respectively. In addition, Ni/SiAl results in higher cracking as there are several peaks in the chromatogram which represent compounds with presumably lower boiling point than methyl palmitate. This suggests a higher cracking ability of Ni/SiAl than CoMo/Al_2O_3. It has been reported that higher acidity of catalyst support causes enhanced cracking of fatty acids and hydrocarbons (Hossain, Chowdhury, Jhawar, Xu, Biesinger, et al. 2018). Therefore, the higher cracking activity of Ni/SiAl than CoMo/Al_2O_3 is possibly due to the higher acidity of SiAl than Al_2O_3 (Sabu, Rao, and Nair 2010).

When the reaction temperature lowers to 220 ^{0}C (Figure 6 *c*), however, Ni/SiAl showed lower conversion and less cracking which indicates that low temperature leads to low cracking and clearly confirms that temperature has significant impact on conversion. Methyl palmitate accounts for 95.71% of the total peak area at 220 ^{0}C and 60.80% at 270 ^{0}C. Thus, higher temperatures are used to increase the yield and conversion of lipids (J. K. Satyarthi, T. Chiranjeevi 2013). A study made by A. Alsobaai et al. also demonstrates that conversion of fatty acids increases with reaction temperature (Alsobaai et al. 2012).

The effect of reaction time on conversion shown in Figure 18 and Figure 19 (Appendix) of Ni/SiAl and CoMo/Al_2O_3 catalyzed pyrolytic reactions, respectively, also show that the conversion is incomplete for both catalysts despite increasing the reaction time from 2 hours to 4 hours. This is in agreement with the FTIR results given in Figure 12 and Figure 13 for the products of Ni/SiAl and CoMo/Al_2O_3catalyzed pyrolytic reactions, respectively, in which a peak characteristic to C=O bond stretching of fatty acids appears in all spectra (Figure 12 and Figure 13). One of the reasons for low conversion of palmitic acid even at extended reaction time could stem from the low catalytic activity at the studied reaction conditions. The low conversion could also be due to low metal loading on the support. J. Wu et al studied the effects of nickel loading on activated carbon and discovered that as the metal loading increased from 10 to 30% conversion of stearic acid increased from 25 to 60% (Wu et al. 2016). It is frequently reported that increasing the amount of

catalyst results in increased catalytic activity since more catalytic sites are available for the reactants (Khan et al. 2019b). However, excessive amount of catalyst could lead to over-cracking (Sudhakara Reddy Yenumala, Sunil K. Maity 2015).

Despite the low conversion, cracking of palmitic acid is noticed at all studied conditions. All chromatograms show a peak at ~5.1 min retention time which suggests the occurrence of cracking of palmitic acid resulting in production of a smaller compound with higher volatility than methyl palmitate. Even though this substance was not identified with the used standard, its boiling point falls between that of methyl octanoate and methyl decanoate, indicating the presence of cracked products. However, further analysis with other analytical tools is necessary to verify the type of the compound. Only two peaks are present in the products of $CoMo/Al_2O_3$ catalyzed pyrolytic reaction products (i.e., at~11.65 min for palmitic acid and ~5.1 min for unknown compound).

Many of the peaks of appearing in GC-FID chromatograms were not assigned due to the large deviation of the retention times of the substances in the sample from the retention times of standard except for methyl decanoate ($C_{21}H_{22}O_2$) whose retention time appears at ~5.4 min in products of Ni/SiAl catalyzed pyrolytic reaction. It can be inferred that decanoic acid ($C_{10}H_{20}O_2$) was produced by Ni/SiAl as a result of palmitic acid cracking. The production of decanoic acid from palmitic acid indicates that some hydrocarbons, such as hexane, pentane, butane, and others were also formed. However, these are volatile compounds, hence lost during evaporation under the fume hood. Complete analysis of the composition of the products was not made due to the limitations with respect to availability of other analytical tools, particularly GC-MS.

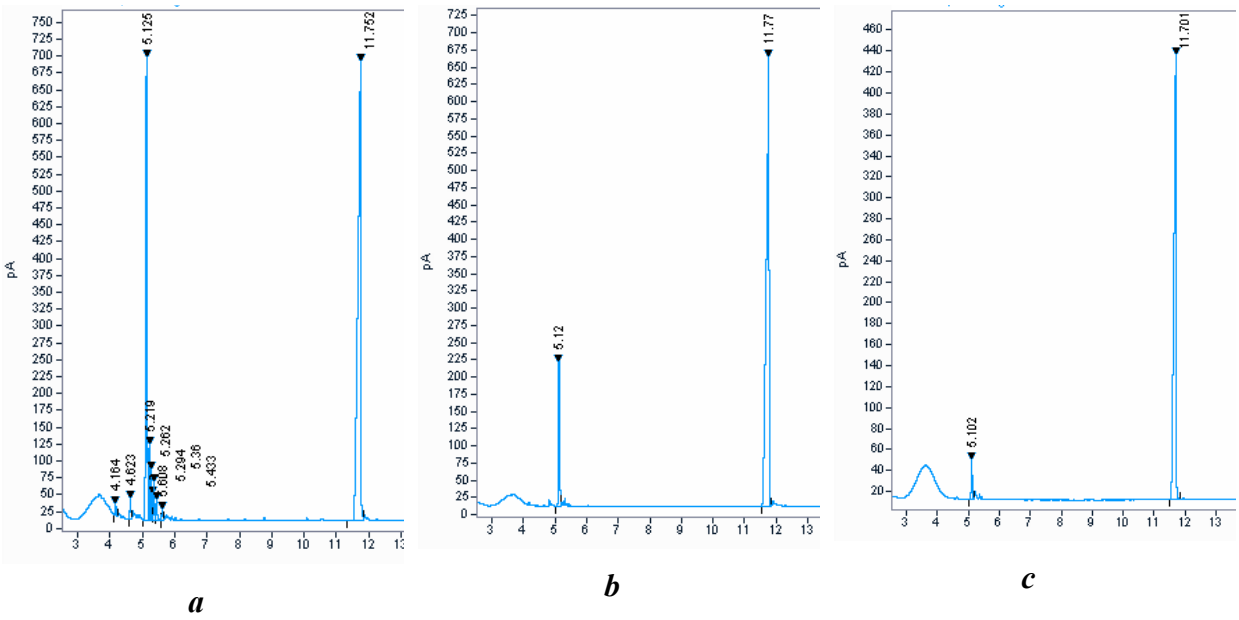

*Figure 6: GC-FID chromatogram of products from (**a.** Ni/SiAl catalyzed pyrolytic reaction (Temp=270 ^{0}C, catalyst loading=16wt%, Time=3hrs) **b.** CoMo/Al_2O_3 catalyzed pyrolytic reaction (Temp=270 ^{0}C, catalyst loading=16wt%, Time=3hrs) **c.** Ni/SiAl catalyzed pyrolytic reaction (Temp=220 ^{0}C, catalyst loading=16wt%, Time=3hrs)*

The following figure (Figure 7) shows the comparison of GC-FID chromatograms of products from Pt/C catalyzed pyrolytic reaction at 8wt% and 12wt% catalyst loading. As can be seen from the figure, methyl palmitate is present in both chromatograms (i.e., peak at ~11.6 min) which indicates that both 8wt% and 12wt% of catalyst loading do not give 100% of conversion of palmitic acid. However, it is obvious from the figure that higher catalyst loading resulted in higher conversion of palmitic acid. The peak area of methyl palmitate accounts for 0.70% and 27.44% of the total area of peaks at 12wt% and 8wt% catalyst loading, respectively. In addition, high cracking can be observed when the catalyst loading increased from 8 to 12wt% which led to the production of several compounds that have higher volatility than methyl palmitate, as shown in the chromatogram (Figure 7 ***b***). Therefore, a 33% difference in Pt/C catalyst loading could result in a significant variation in conversion and degree of cracking.

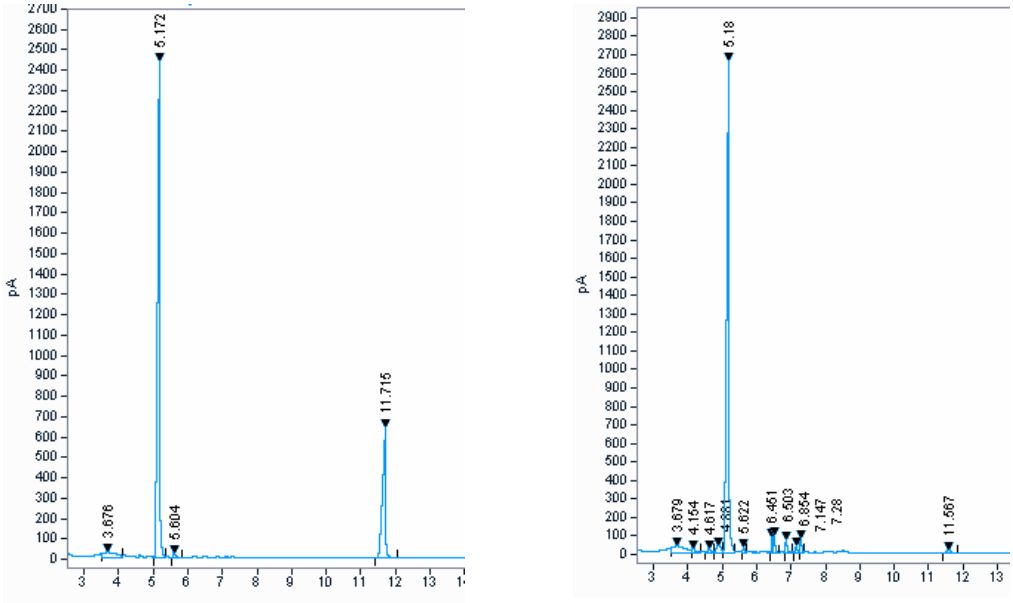

a ***b***

*Figure 7: GC-FID of products from Pt/C catalyzed pyrolytic reaction at 270 ^{0}C, 2h, different loading (**a**=8wt% loading, **b**=12wt% loading)*

The study on the effect of presence of water on conversion shows that water leads to very low conversion of palmitic acid (Figure 8***b***) at the studied reaction conditions (i.e., temperature 270 ^{0}C, 16wt% catalyst loading, and time=1h) as compared to pyrolytic reaction. There was no significant difference in the chromatograms of the products when water was present in the reaction, even when the reaction duration was increased to 3 hours. (Figure 21). Unlike reaction in water, however, pyrolysis gives 100% conversion when the reaction time is increased from 1 to 2 hours. According to a study by B. Jang et al., high conversion of palmitic acid can be attained in the presence of water using 5% Pt/C at near or supercritical water (Jang et al. 2010). Hence, the low conversion obtained in this study may be due to very low reaction temperature (i.e., 270 ^{0}C) compared to supercritical temperature of water. The absence of stirring could also lead to lower conversion of palmitic as mixing allows better heat and mass transfer between the reaction mixture (Khan et al. 2019b).

Water also resulted in low cracking of palmitic acid as there is only one unidentified product having lower boiling point than methyl palmitate (shown in Figure 8***b***). Furthermore, the presence of water caused sticking of the reaction mixture to the reactor wall and tubes leading to low recovery of product and major cleaning issues. This necessitated the frequent cleaning of the reactor using water, electricity, and chemicals resulting in increased downtime and overall cost of

the process. On the other hand, reaction in the absence of water (i.e., pyrolysis) causes less sticking of the reaction mixture to the reactor wall and tubes and gives higher conversion of palmitic acid as compared to reaction in water (i.e., a smaller peak of methyl palmitate in Figure 8***a***). In addition, pyrolysis produced a lot of compounds with lower boiling point than palmitic acid, including decanoic acid (Figure 8 ***a***) which appear at retention times of 5-8 min.

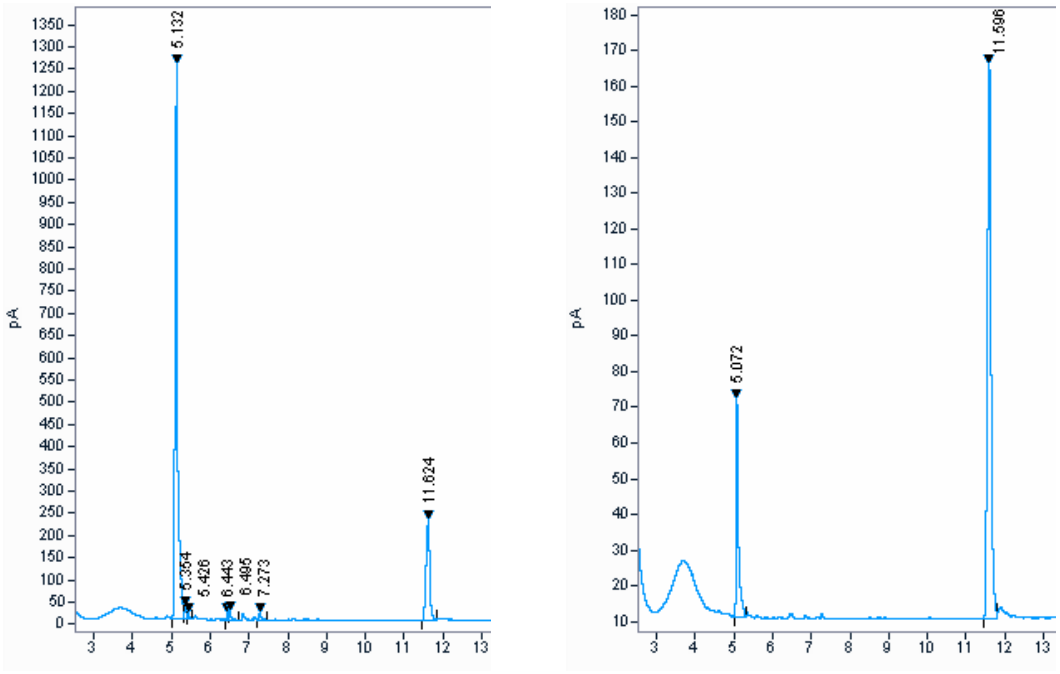

*Figure 8: GC-FID of products from Pt/C catalyzed (**a**) pyrolytic reaction and (**b**) reaction in water (at 270 ^{0}C, 1h, and 16% catalyst loading)*

iii. Hydrocarbon analysis

The liquid products from Pt/C catalyzed pyrolytic reaction (at reaction temperature =270 ^{0}C, catalyst loading of 16wt%, and time= 2h, 3h, and 4h) were analyzed using GC-FID to investigate and prove the presence of hydrocarbons and compare the effect of reaction time on the composition of these hydrocarbons. In addition, in the analysis of fatty acids of many samples, there were several substances with lower boiling point than methyl palmitate but were not identified due to the large variation of retention times of these substances from the retention times in the standard. We hypothesized that those compounds could be hydrocarbons. Hence, a representative sample from Pt/C catalyzed pyrolytic reaction (Temperature: 270 ^{0}C, Reaction time: 2h, catalyst loading: 12wt%) was chosen and subjected to hydrocarbon analysis. The results given in Figure 9 below and Figure 22 (Appendix)), however, show that only pentadecane is present in all the analyzed

samples. The retention times of the small peaks appearing before pentadecane were also not identified as these retention times are missing in the standard. Further analysis, like GC-MS could have been undertaken to fully determine the exact composition of the liquid products.

As discussed above in Figure 4, Pt/C gives complete deoxygenation of palmitic acid at 2 hours of reaction time. Further increase of the reaction time would lead cracking of the hydrocarbons. The effect of the three reaction times on the concentration of pentadecane shown in Figure 9 indicates there is a high peak for pentadecane in all chromatograms with varying concentration of pentadecane which accounts for 98.40%, 94.36%, and 95.94% of the total peak area at 2, 3, and 4 hours respectively. The peak area percentages are the average values of duplicates. Peak areas above 1% are considered significant. The decrease in the concentration of pentadecane as the reaction time increased from 2 to 3 hours implies the presence of cracking at extended reaction time. However, a small increase in concentration of pentadecane is observed when the reaction time is further increased from 3 to 4 hours. This may be due to the further over-cracking of the other compounds at extended reaction time leading to production of volatile compounds which results in higher percentage composition of pentadecane. Nevertheless, the statistical analysis shows that the difference in the area percentage of pentadecane at different reaction time are statistically insignificant at 95% confidence level (p value >0.05). Hence, the reaction time has no significance effect on concentration of pentadecane at the studied conditions.

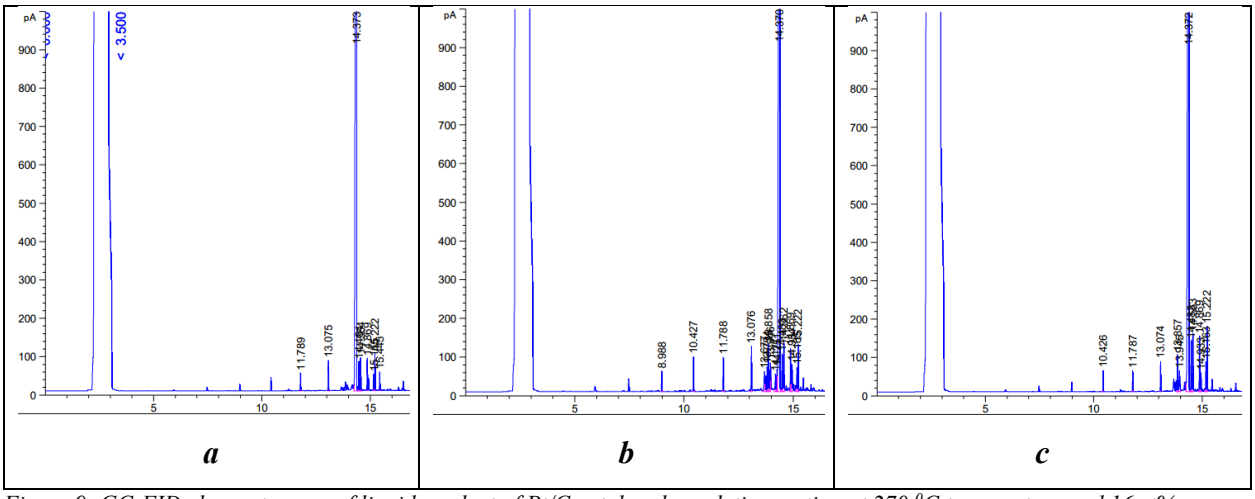

*Figure 9: GC-FID chromatogram of liquid product of Pt/C catalyzed pyrolytic reaction at 270 ^{0}C temperature and 16wt% catalyst loading and different reaction time (**a**=2h, **b**=3h, and **c**=4h)*

From the results, it can be assumed that either decarboxylation or decarbonylation of palmitic acid has taken place resulting in a hydrocarbon with one carbon less than the original fatty acid (i.e., palmitic acid). However, no conclusion can be made regarding the main reaction pathway.

More data about the composition of the solid and liquid products may be obtained using other analytical tools such as GC-MS. Analyzing the gas product may also help in a better understanding of the deoxygenation pathway and overall quantitative analysis. With the available analytical tools, only a few compounds in the product mixture were identified. These constraints led to only partial comparison of the studied catalysts. Nevertheless, very promising results were obtained, specifically with Pt/C. Over 90% pentadecane is obtained using Pt/C. The major product, pentadecane, is a hydrocarbon with a carbon length that falls within the jet fuel range hydrocarbons. Jet fuels, on the other hand, often contain 20% paraffins. This suggests that further cracking and isomerization of pentadecane is necessary to produce iso-paraffins, naphthene and aromatics. This could be achieved either using high reaction temperature and optimum catalyst loading. Expanding the scope of the study to explore the effects of temperature, stirring, catalyst reduction, etc. will help in a better understanding the reaction mechanism and assessment of how catalyst activity changes as a result of these variables.

Conclusion and perspectives

Pyrolysis of palmitic acid were performed using low-cost process (i.e., at relatively low temperature, 6.5 bar of N_2, and no external supply of hydrogen) to evaluate the performance of three catalysts, namely Pt/C, CoMo/Al_2O_3, and Ni/SiAl based on the degree of conversion and liquid yield. The results revealed that Pt/C gives 100% conversion at 2 hours of reaction time and temperature of 270 ^{0}C while the other two catalysts give no liquid product irrespective of the reaction time, although, small degree of conversion was observed. Ni/SiAl showed high cracking activity than CoMo/ Al_2O_3 resulting in several compounds with high volatility than palmitic acid, such as decanoic acid. Hence, the activity of the catalysts is in the order of Pt/C>Ni/SiAl>CoMo/ Al_2O_3.

Although complete analysis was not carried out due to the above-mentioned limitations, Pt/C showed very high catalytic activity at relatively mild temperature without addition of external hydrogen. The most challenging part in using Pt/C for large scale production of bio-jet fuel is the high cost of the catalyst. In this regard, reusing the catalyst may reduce the cost of the process. Thus, comprehensive research aimed at finding methods of improving the reusability the catalyst is vital to overcome these challenges.

Résumé

L'inquiétude croissante concernant l'épuisement des combustibles fossiles et la pollution de l'environnement due principalement au secteur du transport a forcé la recherche de carburants alternatifs renouvelables. La pyrolyse est une approche prometteuse pour convertir les lipides en carburants en utilisant des catalyseurs. Dans le présent travail, la désoxygénation catalytique de l'acide palmitique en réacteur sous pression a été étudiée sans apport externe d'hydrogène, afin de comparer la performance de trois catalyseurs, à savoir Pt/C, Ni/SiAl et $CoMo/Al_2O_3$. Les produits de la réaction ont été analysés par FTIR pour vérifier la présence d'acides gras pas convertis. Les échantillons dont FTIR a montré un pic caractéristique de l'étirement C=O (à environ 1708 cm^{-1}) ont été soumis à la détermination d'acide gras par GC-FID. Ceci a été fait pour valider la présence de l'acide résiduel et explorer la présence d'autres acides gras à plus petite chaîne de carbone. Les produits liquides ont également été analysés par GC-FID avec la colonne HP-5 pour confirmer la présence d'hydrocarbures. Les résultats révèlent que le catalyseur à Ni/SiAl a une activité de craquage plus élevée que celui à $CoMo/Al_2O_3$, tandis que le catalyseur à Pt/C montre la meilleure performance donnant une conversion complète de l'acide palmitique à 2 heures et 270 ^{0}C. Le pentadécane était le principal hydrocarbure produit par Pt/C. Les effet du temps de réaction, de la charge du catalyseur et de la présence d'eau sur la conversion ont également été couverts. Les instruments analytiques utilisés n'ont pas permis une identification complète de la composition des produits, donc aucune analyse détaillée du rendement et de la sélectivité n'a pas été réalisée.

Mots-clés : carburéacteur, désoxygénation, pyrolyse, hydrocarbure, pentadécane

References

Ahmadi, M. et al. 2015. “Decarboxylation of Oleic Acid over Pt Catalysts Supported on Small-Pore Zeolites and Hydrotalcite.” *Catalysis Science and Technology* 5(1): 380–88. http://dx.doi.org/10.1039/C4CY00661E.

Alsobaai, Ahmed Mubarak, Abdulmajid Mohammed Al Shaibani, Tarek Moustafa, and Abduljalil Derhem. 2012. “Effect of Hydrogenation Temperature on the Palm Mid-Fraction Fatty Acids Composition and Conversion.” *Journal of King Saud University - Engineering Sciences* 24(1): 45–51. http://dx.doi.org/10.1016/j.jksues.2011.02.004.

Anand, Mohit et al. 2016. “Kinetics, Thermodynamics and Mechanisms for Hydroprocessing of Renewable Oils.” *Applied Catalysis A: General* 516: 144–52. http://dx.doi.org/10.1016/j.apcata.2016.02.027.

Arun, Naveenji, Rajesh V Sharma, and Ajay K Dalai. 2015. “Green Diesel Synthesis by Hydrodeoxygenation of Bio-Based Feedstocks: Strategies for Catalyst Design and Development.” *Renewable and Sustainable Energy Reviews* 48: 240–55. https://www.sciencedirect.com/science/article/pii/S1364032115002270.

Asikin-Mijan, N et al. 2017. “Optimization Study of SiO2-Al2O3 Supported Bifunctional Acid–Base NiO-CaO for Renewable Fuel Production Using Response Surface Methodology.” *Energy Conversion and Management* 141: 325–38. https://www.sciencedirect.com/science/article/pii/S0196890416308317.

Atsonios, Konstantinos, Michael Alexander Kougioumtzis, Kyriakos D. Panopoulos, and Emmanuel Kakaras. 2015. “Alternative Thermochemical Routes for Aviation Biofuels via Alcohols Synthesis: Process Modeling, Techno-Economic Assessment and Comparison.” *Applied Energy* 138: 346–66. http://dx.doi.org/10.1016/j.apenergy.2014.10.056.

Bagheri, Samira, Nurhidayatullaili Muhd Julkapli, and Sharifah Bee Abd Hamid. 2014. “Titanium Dioxide as a Catalyst Support in Heterogeneous Catalysis” ed. Alexander Vorontsov. *The Scientific World Journal* 2014: 727496. https://doi.org/10.1155/2014/727496.

Bernabei, M., R. Reda, R. Galiero, and G. Bocchinfuso. 2003. “Determination of Total and Polycyclic Aromatic Hydrocarbons in Aviation Jet Fuel.” *Journal of Chromatography A* 985(1–2): 197–203.

Biller, Patrick, Brajendra K. Sharma, Bidhya Kunwar, and Andrew B. Ross. 2015. “Hydroprocessing of Bio-Crude from Continuous Hydrothermal Liquefaction of Microalgae.” *Fuel* 159: 197–205.

http://dx.doi.org/10.1016/j.fuel.2015.06.077.

Blakey, Simon, Lucas Rye, and Christopher Willam Wilson. 2011. “Aviation Gas Turbine Alternative Fuels: A Review.” *Proceedings of the Combustion Institute* 33(2): 2863–85. http://dx.doi.org/10.1016/j.proci.2010.09.011.

Chen, Hao et al. 2020. “Highly Efficient Conversion of Oleic Acid to Heptadecane without External Hydrogen Source over Atomic Layer Deposited Bimetallic NiPt Catalysts.” *Chemical Engineering Journal* 390(February): 124603. https://doi.org/10.1016/j.cej.2020.124603.

Cheng, Jun et al. 2019. “Continuous Hydroprocessing of Microalgae Biodiesel to Jet Fuel Range Hydrocarbons Promoted by Ni/Hierarchical Mesoporous Y Zeolite Catalyst.” *International Journal of Hydrogen Energy* 44(23): 11765–73. https://www.sciencedirect.com/science/article/pii/S0360319919310523.

Chiaramonti, David et al. 2016. “Bio-Hydrocarbons through Catalytic Pyrolysis of Used Cooking Oils and Fatty Acids for Sustainable Jet and Road Fuel Production.” *Biomass and Bioenergy* 95: 424–35.

Choi, Il-ho et al. 2015. “The Direct Production of Jet-Fuel from Non-Edible Oil in a Single-Step Process.” *FUEL* (May): 1–7. http://dx.doi.org/10.1016/j.fuel.2015.05.020.

Dayton, David C., and Thomas D. Foust. 2020. “Alternative Jet Fuels.” *Analytical Methods for Biomass Characterization and Conversion*: 147–65.

De, Sudipta, Jiaguang Zhang, Rafael Luque, and Ning Yan. 2016. “Ni-Based Bimetallic Heterogeneous Catalysts for Energy and Environmental Applications.” *Energy and Environmental Science* 9(11): 3314–47.

Díaz-Pérez, Manuel Antonio, and Juan Carlos Serrano-Ruiz. 2020. “Catalytic Production of Jet Fuels from Biomass.” *Molecules* 25(4).

Duan, Peigao et al. 2013. “Catalytic Upgrading of Crude Algal Oil Using Platinum/Gamma Alumina in Supercritical Water.” *Fuel* 109: 225–33. http://dx.doi.org/10.1016/j.fuel.2012.12.074.

Duan, Peigao, and Phillip E. Savage. 2011. “Upgrading of Crude Algal Bio-Oil in Supercritical Water.” *Bioresource Technology* 102(2): 1899–1906. http://dx.doi.org/10.1016/j.biortech.2010.08.013.

Edeh, Ifeanyichukwu, Tim Overton, and Steve Bowra. 2021. “Renewable Diesel Production by Hydrothermal Decarboxylation of Fatty Acids over Platinum on Carbon Catalyst.” *Biofuels* 12(8): 945–52. https://doi.org/10.1080/17597269.2018.1560554.

El-Lateef, Hany. 2013. “Evaluation of New Complex Surfactants Based on Vegetable Oils as Corrosion Inhibitors for Mild Steel in CO 2-Saturated 1.0% NaCl Solutions.” *Journal of Materials Physics and Chemistry* 1: 19–26.

Eller, Zoltán, Zoltán Varga, and Jeno Hancsók. 2016. “Advanced Production Process of Jet Fuel Components from Technical Grade Coconut Oil with Special Hydrocracking.” *Fuel* 182: 713–20.

Elliott, Douglas C, L John Sealock, and Eddie G Baker. 1993. “Chemical Processing in High-Pressure Aqueous Environments. 2. Development of Catalysts for Gasification.” *Industrial & Engineering Chemistry Research* 32(8): 1542–48. https://doi.org/10.1021/ie00020a002.

Faroon, O.M., Mandell, D.M., & Navarro, H.A. 1995. “Toxicological Profile for Jet Fuels (JP4 and JP7).” *ATSDR's Toxicological Profiles* (June).

Feng, Fuxiang, Zeyu Shang, et al. 2020. “Structure-Sensitive Hydro-Conversion of Oleic Acid to Aviation-Fuel-Range-Alkanes over Alumina-Supported Nickel Catalyst.” *Catalysis Communications* 134.

Feng, Fuxiang, Xiaopo Niu, et al. 2020. “TEOS-Modified Ni/ZSM-5 Nanosheet Catalysts for Hydroconversion of Oleic Acid to High-Performance Aviation Fuel: Effect of Acid Spatial Distribution.” *Microporous and Mesoporous Materials* 291.

Fu, Jie et al. 2015. “Direct Production of Aviation Fuels from Microalgae Lipids in Water.” *Fuel* 139: 678–83. http://dx.doi.org/10.1016/j.fuel.2014.09.025.

Fu, Jie, Xiuyang Lu, and Phillip E Savage. 2011. “Hydrothermal Decarboxylation and Hydrogenation of Fatty Acids over Pt/C.” *ChemSusChem* 4(4): 481–86. https://doi.org/10.1002/cssc.201000370.

Galadima, Ahmad, and Oki Muraza. 2015a. “Catalytic Upgrading of Vegetable Oils into Jet Fuels Range Hydrocarbons Using Heterogeneous Catalysts: A Review.” *Journal of Industrial and Engineering Chemistry* 29: 12–23. http://dx.doi.org/10.1016/j.jiec.2015.03.030.

———. 2015b. “Catalytic Upgrading of Vegetable Oils into Jet Fuels Range Hydrocarbons Using Heterogeneous Catalysts: A Review.” *Journal of Industrial and Engineering Chemistry* 29: 12–23. https://www.sciencedirect.com/science/article/pii/S1226086X15001070.

Goh, Brandon Han Hoe et al. 2022. “Recent Advancements in Catalytic Conversion Pathways for Synthetic Jet Fuel Produced from Bioresources.” *Energy Conversion and Management* 251(September 2021).

Han, Yang et al. 2019. “Hydrothermal Liquefaction of Marine Microalgae Biomass Using Co-Solvents.” *Algal Research* 38.

Hansen, Samuel, Amin Mirkouei, and Luis A. Diaz. 2020. “A Comprehensive State-of-Technology Review for Upgrading Bio-Oil to Renewable or Blended Hydrocarbon Fuels.” *Renewable and Sustainable Energy Reviews* 118(June 2019): 109548. https://doi.org/10.1016/j.rser.2019.109548.

Hemighaus, Greg et al. 2006. “Aviation Fuels Technical Review.” *Chevron Corporation*.

Hileman, J. I., and R. W. Stratton. 2014. “Alternative Jet Fuel Feasibility.” *Transport Policy* 34: 52–62. http://dx.doi.org/10.1016/j.tranpol.2014.02.018.

Hossain, Md Zakir, Muhammad B.I. Chowdhury, Anil Kumar Jhawar, William Z. Xu, Mark C. Biesinger, et al. 2018. “Continuous Hydrothermal Decarboxylation of Fatty Acids and Their Derivatives into Liquid Hydrocarbons Using Mo/Al2O3 Catalyst.” *ACS Omega* 3(6): 7046–60.

Hossain, Md Zakir, Muhammad B.I. Chowdhury, Anil Kumar Jhawar, William Z. Xu, and Paul A. Charpentier. 2018. “Continuous Low Pressure Decarboxylation of Fatty Acids to Fuel-Range Hydrocarbons with in Situ Hydrogen Production.” *Fuel* 212(September 2017): 470–78. http://dx.doi.org/10.1016/j.fuel.2017.09.092.

Hwang, Kyung Ran et al. 2016. “Bio Fuel Production from Crude Jatropha Oil; Addition Effect of Formic Acid as an in-Situ Hydrogen Source.” *Fuel* 174: 107–13. http://dx.doi.org/10.1016/j.fuel.2016.01.080.

Itthibenchapong, Vorranutch et al. 2017. “Deoxygenation of Palm Kernel Oil to Jet Fuel-like Hydrocarbons Using Ni-MoS2/γ-Al2O3catalysts.” *Energy Conversion and Management* 134: 188–96. http://dx.doi.org/10.1016/j.enconman.2016.12.034.

J. K. Satyarthi, T. Chiranjeevi, D. T. Gokak and P. S. Viswanathan. 2013. “An Overview of Catalytic Conversion of Vegetable Oils/Fats into Middle Distillates.” (c): 70–80.

Jamil, Farrukh et al. 2017. “Phoenix Dactylifera Kernel Oil Used As Potential Source for Synthesizing Jet Fuel and Green Diesel.” *Energy Procedia* 118: 35–39. http://dx.doi.org/10.1016/j.egypro.2017.07.006.

Janampelli, Sagar, and Srinivas Darbha. 2021. “Selective Deoxygenation of Fatty Acids to Fuel-Range Hydrocarbons over Pt-MOx/ZrO2 (M = Mo and W) Catalysts.” *Catalysis Today* 375: 174–80. https://www.sciencedirect.com/science/article/pii/S092058612030208X.

Jang, Ben W.L., Roger Gläser, Mingdong Dong, and Chang Jun Liu. 2010. “Catalytic Hydrothermal Deoxygenation of Palmitic Acid.” *Energy and Environmental Science* 3(3): 253.

Jaroszewska, Karolina et al. 2014. “Effect of Support Composition on the Activity of Pt and PtMo Catalysts in the Conversion of N-Hexadecane.” *Catalysis Today* 223: 76–86. http://dx.doi.org/10.1016/j.cattod.2013.07.010.

Jia, Chuhua et al. 2021. “One-Pot Production of Jet Fuels from Fatty Acids and Vegetable Oils in Biphasic Tandem Catalytic Process.” *Fuel* 302(March): 121060. https://doi.org/10.1016/j.fuel.2021.121060.

Khan, Saima et al. 2019a. “A Review on Deoxygenation of Triglycerides for Jet Fuel Range Hydrocarbons.” *Journal of Analytical and Applied Pyrolysis* 140(November 2018): 1–24. https://doi.org/10.1016/j.jaap.2019.03.005.

———. 2019b. “A Review on Deoxygenation of Triglycerides for Jet Fuel Range Hydrocarbons.” *Journal of Analytical and Applied Pyrolysis* 140(March): 1–24. https://doi.org/10.1016/j.jaap.2019.03.005.

Konwar, Lakhya Jyoti, and Jyri-Pekka Mikkola. 2022. “Carbon Support Effects on Metal (Pd, Pt and Ru) Catalyzed Hydrothermal Decarboxylation/Deoxygenation of Triglycerides.” *Applied Catalysis A: General* 638(January): 118611. https://doi.org/10.1016/j.apcata.2022.118611.

Kubička, David. 2008. “Future Refining Catalysis - Introduction of Biomass Feedstocks.” *Collection of Czechoslovak Chemical Communications* 73(8–9): 1015–44.

Lestari, Siswati et al. 2009. “Catalytic Deoxygenation of Stearic Acid and Palmitic Acid in Semibatch Mode.” *Catalysis Letters* 130: 48–51.

Li, Dan et al. 2015. “Recent Advances for the Production of Hydrocarbon Biofuel via Deoxygenation Progress.” *Science Bulletin* 60(24): 2096–2106. https://www.sciencedirect.com/science/article/pii/S2095927316302390.

Li, Jing et al. 2018. “Microalgae Hydrothermal Liquefaction and Derived Biocrude Upgrading with Modified SBA-15 Catalysts.” *Bioresource Technology* 266: 541–47.

Li, Tao et al. 2015. “Conversion of Waste Cooking Oil to Jet Biofuel with Nickel-Based Mesoporous Zeolite Y Catalyst.” *Bioresource Technology* 197: 289–94. https://www.sciencedirect.com/science/article/pii/S0960852415012213.

Lim, Jackson Hwa Keen et al. 2021. “Utilization of Microalgae for Bio-Jet Fuel Production in the

Aviation Sector: Challenges and Perspective." *Renewable and Sustainable Energy Reviews* 149.

Liu, Guangrui, Beibei Yan, and Guanyi Chen. 2013. "Technical Review on Jet Fuel Production." *Renewable and Sustainable Energy Reviews* 25: 59–70. http://dx.doi.org/10.1016/j.rser.2013.03.025.

Liu, Qiying et al. 2014. "Hydrodeoxygenation of Palm Oil to Hydrocarbon Fuels over Ni/SAPO-11 Catalysts." *Cuihua Xuebao/Chinese Journal of Catalysis* 35(5): 748–56. http://dx.doi.org/10.1016/S1872-2067(12)60710-4.

Lokesh, Kadambari et al. 2015. "Life Cycle Greenhouse Gas Analysis of Biojet Fuels with a Technical Investigation into Their Impact Onjet Engine Performance." *Biomass and Bioenergy* 77: 26–44. http://dx.doi.org/10.1016/j.biombioe.2015.03.005.

Madsen, Anders Theilgaard et al. 2011. "Hydrodeoxygenation of Waste Fat for Diesel Production: Study on Model Feed with Pt/Alumina Catalyst." *Fuel* 90(11): 3433–38. http://dx.doi.org/10.1016/j.fuel.2011.06.005.

Martinez-Hernandez, Elias, Luis Felipe Ramírez-Verduzco, Myriam A. Amezcua-Allieri, and Jorge Aburto. 2019. "Process Simulation and Techno-Economic Analysis of Bio-Jet Fuel and Green Diesel Production — Minimum Selling Prices." *Chemical Engineering Research and Design* 146: 60–70. https://doi.org/10.1016/j.cherd.2019.03.042.

Miao, Chao et al. 2016. "Hydrothermal Catalytic Deoxygenation of Palmitic Acid over Nickel Catalyst." *Fuel* 166: 302–8.

Mo, Ni et al. 2009. "Hydrotreatment of Jatropha Oil to Produce Green Diesel." 38(6): 552–53.

Murata, Kazuhisa, Yanyong Liu, Megumu Inaba, and Isao Takahara. 2010. "Production of Synthetic Diesel by Hydrotreatment of Jatropha Oils Using Pt−Re/H-ZSM-5 Catalyst." *Energy & Fuels* 24(4): 2404–9. https://doi.org/10.1021/ef901607t.

Nam, Hyungseok, Changkyu Kim, Sergio C. Capareda, and Sushil Adhikari. 2017. "Catalytic Upgrading of Fractionated Microalgae Bio-Oil (Nannochloropsis Oculata) Using a Noble Metal (Pd/C) Catalyst." *Algal Research* 24: 188–98. http://dx.doi.org/10.1016/j.algal.2017.03.021.

Nishida, Jun, Shinsuke Shigeto, Sohshi Yabumoto, and Hiro O. Hamaguchi. 2012. "Anharmonic Coupling of the CH-Stretch and CH-Bend Vibrations of Chloroform as Studied by near-Infrared Electroabsorption Spectroscopy." *Journal of Chemical Physics* 137(23).

Nosal, Hanna et al. 2021. "Selected Fatty Acids Esters as Potential PHB-V Bioplasticizers: Effect on

Mechanical Properties of the Polymer." *Journal of Polymers and the Environment* 29.

Osada, Mitsumasa, Osamu Sato, Kunio Arai, and Masayuki Shirai. 2006. "Stability of Supported Ruthenium Catalysts for Lignin Gasification in Supercritical Water." *Energy & Fuels* 20(6): 2337–43. https://doi.org/10.1021/ef060356h.

Oubagaranadin, John, and Z V P Murthy. 2011. "Activated Carbons: Classifications, Properties and Applications." *Activated Carbon: Classifications, Properties and Applications*: 239–66.

Panarmasar, N., N. Hinchiranan, and P. Kuchonthara. 2021. "Catalytic Hydrotreating of Palm Oil for Bio-Jet Fuel Production over Ni Supported on Mesoporous Zeolite." *Materials Today: Proceedings* (xxxx). https://doi.org/10.1016/j.matpr.2021.09.385.

Peng, Baoxiang et al. 2013. "Manipulating Catalytic Pathways: Deoxygenation of Palmitic Acid on Multifunctional Catalysts." *Chemistry - A European Journal* 19(15): 4732–41.

Phichitsurathaworn, Ploynisa, Kittisak Choojun, Yingyot Poo-arporn, and Tawan Sooknoi. 2020. "Deoxygenation of Heptanoic Acid to Hexene over Cobalt-Based Catalysts: A Model Study for α-Olefin Production from Renewable Fatty Acid." *Applied Catalysis A: General* 602: 117644. https://www.sciencedirect.com/science/article/pii/S0926860X20302374.

Rabaev, Moshe et al. 2015. "Conversion of Vegetable Oils on Pt/Al2O3/SAPO-11 to Diesel and Jet Fuels Containing Aromatics." *Fuel* 161: 287–94. http://dx.doi.org/10.1016/j.fuel.2015.08.063.

Rafiani, A. et al. 2020. "Studies on Nickel-Based Bimetallic Catalysts for the Hydrodeoxygenation of Stearic Acid." *IOP Conference Series: Materials Science and Engineering* 722(1).

Ren, Rui et al. 2018. "High Yield Bio-Oil Production by Hydrothermal Liquefaction of a Hydrocarbon-Rich Microalgae and Biocrude Upgrading." *Carbon Resources Conversion* 1(2): 153–59. https://doi.org/10.1016/j.crcon.2018.07.008.

Romero, M. J.A. et al. 2016. "Deoxygenation of Waste Cooking Oil and Non-Edible Oil for the Production of Liquid Hydrocarbon Biofuels." *Waste Management* 47: 62–68. http://dx.doi.org/10.1016/j.wasman.2015.03.033.

Roy, Poulami et al. 2022. "Performance of Biochar Assisted Catalysts during Hydroprocessing of Non-Edible Vegetable Oil: Effect of Transition Metal Source on Catalytic Activity." *Energy Conversion and Management* 252(December): 115131. https://doi.org/10.1016/j.enconman.2021.115131.

Sabu, K. R. P., K. V. C. Rao, and C. G. R. Nair. 2010. "ChemInform Abstract: A Comparative Study on

the Acidic Properties and Catalytic Activities of TiO2, SiO2, Al2O3, SiO2-Al2O3, SiO2-TiO2, Al2O3-TiO2, and TiO2-SiO2- Al2O3." *ChemInform* 22(38): no-no.

Salimon, Jumat, Nadia Salih, and Bashar Mudhaffar Abdullah. 2011. "Improvement of Physicochemical Characteristics of Monoepoxide Linoleic Acid Ring Opening for Biolubricant Base Oil." *Journal of Biomedicine and Biotechnology* 2011.

Sanna, Aimaro, Tushar P. Vispute, and George W. Huber. 2015. "Hydrodeoxygenation of the Aqueous Fraction of Bio-Oil with Ru/C and Pt/C Catalysts." *Applied Catalysis B: Environmental* 165(April): 446–56. http://dx.doi.org/10.1016/j.apcatb.2014.10.013.

Satyarthi, J. K., T. Chiranjeevi, D. T. Gokak, and P. S. Viswanathan. 2013. "An Overview of Catalytic Conversion of Vegetable Oils/Fats into Middle Distillates." *Catalysis Science and Technology* 3(1): 70–80.

Scaldaferri, Cristiane Almeida, and Vânya Márcia Duarte Pasa. 2019. "Hydrogen-Free Process to Convert Lipids into Bio-Jet Fuel and Green Diesel over Niobium Phosphate Catalyst in One-Step." *Chemical Engineering Journal* 370(November 2018): 98–109. https://doi.org/10.1016/j.cej.2019.03.063.

Shakya, Rajdeep et al. 2018. "Catalytic Upgrading of Bio-Oil Produced from Hydrothermal Liquefaction of Nannochloropsis Sp." *Bioresource Technology* 252: 28–36. https://doi.org/10.1016/j.biortech.2017.12.067.

Silva, Larissa Noemí, Isabel C.P. Fortes, Fabiana P. De Sousa, and Vânya M.D. Pasa. 2016. "Biokerosene and Green Diesel from Macauba Oils via Catalytic Deoxygenation over Pd/C." *Fuel* 164: 329–38.

Simakova, Irina et al. 2009. "Deoxygenation of Palmitic and Stearic Acid over Supported Pd Catalysts: Effect of Metal Dispersion." *Applied Catalysis A: General* 355(1): 100–108. https://www.sciencedirect.com/science/article/pii/S0926860X08007527.

Snåre, Mathias et al. 2006a. "Heterogeneous Catalytic Deoxygenation of Stearic Acid for Production of Biodiesel." *Industrial and Engineering Chemistry Research* 45(16): 5708–15.

———. 2006b. "Heterogeneous Catalytic Deoxygenation of Stearic Acid for Production of Biodiesel." *Industrial & Engineering Chemistry Research - IND ENG CHEM RES* 45.

Soni, Vineet Kumar et al. 2017. "Ni/Co-Natural Clay as Green Catalysts for Microalgae Oil to Diesel-Grade Hydrocarbons Conversion." *ACS Sustainable Chemistry and Engineering* 5(6): 5351–59.

De Sousa, Fabiana P., Claudia C. Cardoso, and Vânya M.D. Pasa. 2016. "Producing Hydrocarbons for

Green Diesel and Jet Fuel Formulation from Palm Kernel Fat over Pd/C." *Fuel Processing Technology* 143: 35–42. http://dx.doi.org/10.1016/j.fuproc.2015.10.024.

de Sousa, Fabiana P, Claudia C Cardoso, and Vânya M D Pasa. 2016. "Producing Hydrocarbons for Green Diesel and Jet Fuel Formulation from Palm Kernel Fat over Pd/C." *Fuel Processing Technology* 143: 35–42. https://www.sciencedirect.com/science/article/pii/S0378382015302113.

Srifa, Atthapon et al. 2014. "Production of Bio-Hydrogenated Diesel by Catalytic Hydrotreating of Palm Oil over NiMoS2/γ-Al2O3 Catalyst." *Bioresource Technology* 158: 81–90. http://dx.doi.org/10.1016/j.biortech.2014.01.100.

Srifa, Atthapon, Kajornsak Faungnawakij, Vorranutch Itthibenchapong, and Suttichai Assabumrungrat. 2015. "Roles of Monometallic Catalysts in Hydrodeoxygenation of Palm Oil to Green Diesel." *Chemical Engineering Journal* 278: 249–58. http://dx.doi.org/10.1016/j.cej.2014.09.106.

Sudhakara Reddy Yenumala, Sunil K. Maity, and Debaprasad Shee. 2015. "Hydrodeoxygenation of Karanja Oil over Supported Nickel Catalysts: Influence of Support and Nickel Loading."

Tian, Qiurong et al. 2016. "Direct Production of Aviation Fuel Range Hydrocarbons and Aromatics from Oleic Acid without an Added Hydrogen Donor Direct Production of Aviation Fuel Range Hydrocarbons and Aromatics from Oleic Acid without an Added Hydrogen Donor."

Timko, Michael T. et al. 2011. "Combustion Products of Petroleum Jet Fuel, a Fischer-Tropsch Synthetic Fuel, and a Biomass Fatty Acid Methyl Ester Fuel for a Gas Turbine Engine." *Combustion Science and Technology* 183(10): 1039–68.

Toba, Makoto et al. 2011. "Hydrodeoxygenation of Waste Vegetable Oil over Sulfide Catalysts." *Catalysis Today* 164(1): 533–37. http://dx.doi.org/10.1016/j.cattod.2010.11.049.

Venter, Roelf, Corneels Schabort, and Sanette Marx. 2015. "The Hydrotreatment of an Unsaturated Fatty Acid Vegetable Oil To Hydrocarbons Over Ni/Sio2 - Al(2)O(3)." *Papers of the 23Rd European Biomass Conference: Setting the Course for a Biobased Economy* (June): 970–73.

Veriansyah, Bambang et al. 2012. "Production of Renewable Diesel by Hydroprocessing of Soybean Oil: Effect of Catalysts." *Fuel* 94: 578–85. http://dx.doi.org/10.1016/j.fuel.2011.10.057.

Votano, JR, M Parham, and LH Hall. 2004. "Infrared Spectroscopy Table." *Chemistry & ...*: 1–4. http://onlinelibrary.wiley.com/doi/10.1002/cbdv.200490137/abstract.

Watanabe, Masaru, Toru Iida, and Hiroshi Inomata. 2006. "Decomposition of a Long Chain Saturated

Fatty Acid with Some Additives in Hot Compressed Water." *Energy Conversion and Management* 47(18–19): 3344–50.

Wei, Hongjian et al. 2019. "Renewable Bio-Jet Fuel Production for Aviation: A Review." *Fuel* 254(June).

Wildschut, Jelle, Farchad H Mahfud, Robbie H Venderbosch, and Hero J Heeres. 2009. "Hydrotreatment of Fast Pyrolysis Oil Using Heterogeneous Noble-Metal Catalysts Jelle." : 10324–34.

William W. Christie, Xianlin Han. 2012. "Lipids : Their Structures and Occurrence." : 3–19.

Wu, Jianghua et al. 2016. "Catalytic Decarboxylation of Fatty Acids to Aviation Fuels over Nickel Supported on Activated Carbon." *Scientific reports* 6: 27820. https://pubmed.ncbi.nlm.nih.gov/27292280.

Xu, Donghai et al. 2019. "Hydrothermal Upgrading of Water-Insoluble Algal Biocrude over Γ-Al2O3 Supported Multi-Metallic Catalysts." *Journal of Analytical and Applied Pyrolysis* 140(March): 188–94. https://doi.org/10.1016/j.jaap.2019.03.014.

Xu, Junming, Jianchun Jiang, and Jiaping Zhao. 2016. "Thermochemical Conversion of Triglycerides for Production of Drop-in Liquid Fuels." *Renewable and Sustainable Energy Reviews* 58: 331–40. http://dx.doi.org/10.1016/j.rser.2015.12.315.

Xu, Yuping, Peigao Duan, and Bing Wang. 2015. "Catalytic Upgrading of Pretreated Algal Oil with a Two-Component Catalyst Mixture in Supercritical Water." *Algal Research* 9: 186–93. http://dx.doi.org/10.1016/j.algal.2015.03.011.

Zarchin, Ruby et al. 2015. "Hydroprocessing of Soybean Oil on Nickel-Phosphide Supported Catalysts." *Fuel* 139: 684–91. http://dx.doi.org/10.1016/j.fuel.2014.09.053.

Zhao, Xianhui, Lin Wei, Shouyun Cheng, and James Julson. 2017. "Review of Heterogeneous Catalysts for Catalytically Upgrading Vegetable Oils into Hydrocarbon Biofuels." *Catalysts* 7(3).

Zhao, Xuebing, Xiaoying Sun, Xingkai Cui, and Dehua Liu. 2019. "Production of Biojet Fuels from Biomass." In *Sustainable Bioenergy: Advances and Impacts*, Elsevier, 127–65.

Zhong, Heng et al. 2019. 209 Journal of Cleaner Production *Non-Precious Metal Catalyst, Highly Efficient Deoxygenation of Fatty Acids to Alkanes with in Situ Hydrogen from Water*. Elsevier Ltd. https://doi.org/10.1016/j.jclepro.2018.10.318.

Appendix

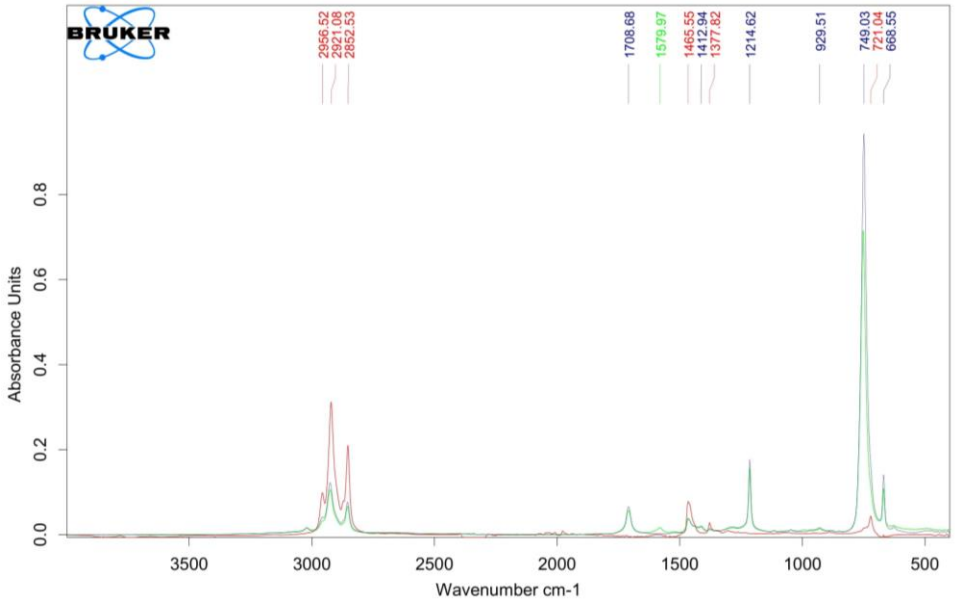

Figure 10: FTIR of Pt/C catalyzed (red), Ni/SiAl catalyzed (blue) and CoMo/Al_2O_3 catalyzed (light green) products. (Reaction time= 3h, temperature= 270 ^{0}C, catalyst loading=16wt%)

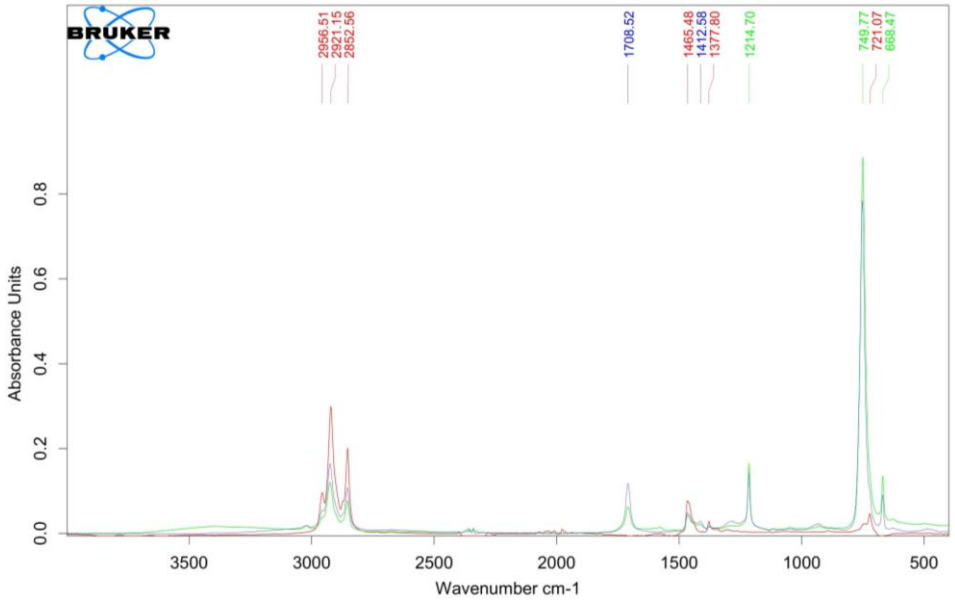

Figure 11: FTIR of Pt/C catalyzed (red), Ni/SiAl catalyzed (blue) and CoMo/Al_2O_3 catalyzed (light green) pyrolytic products. (reaction time= 4h, temperature= 270 ^{0}C, catalyst loading=16wt%)

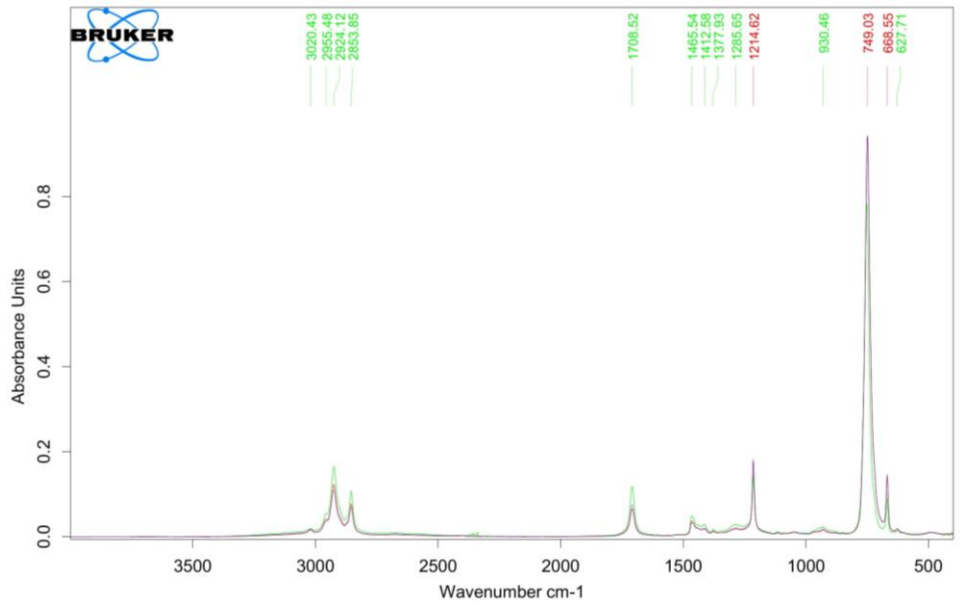

Figure 12: FTIR spectra of Ni/SiAl catalyzed pyrolytic product at 270 ^{0}C and 16% catalyst loading (reaction time=>blue=2h, red=3h, and light green=4h).

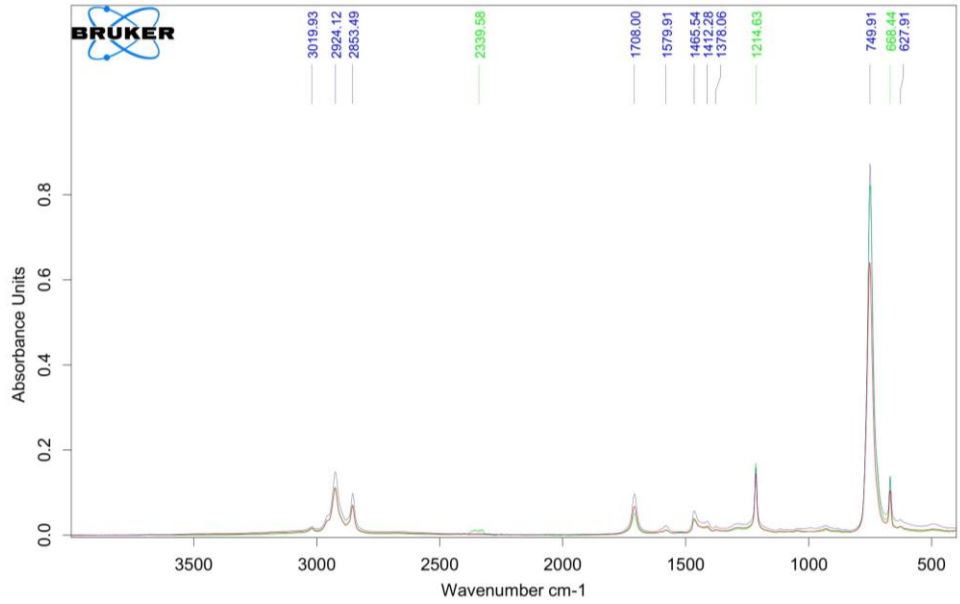

Figure 13: FTIR spectra of CoMo/Al_2O_3 catalyzed pyrolytic product at 270 ^{0}C and 16% catalyst loading (residence time=>blue=2h, red=3h, and light green=4h).

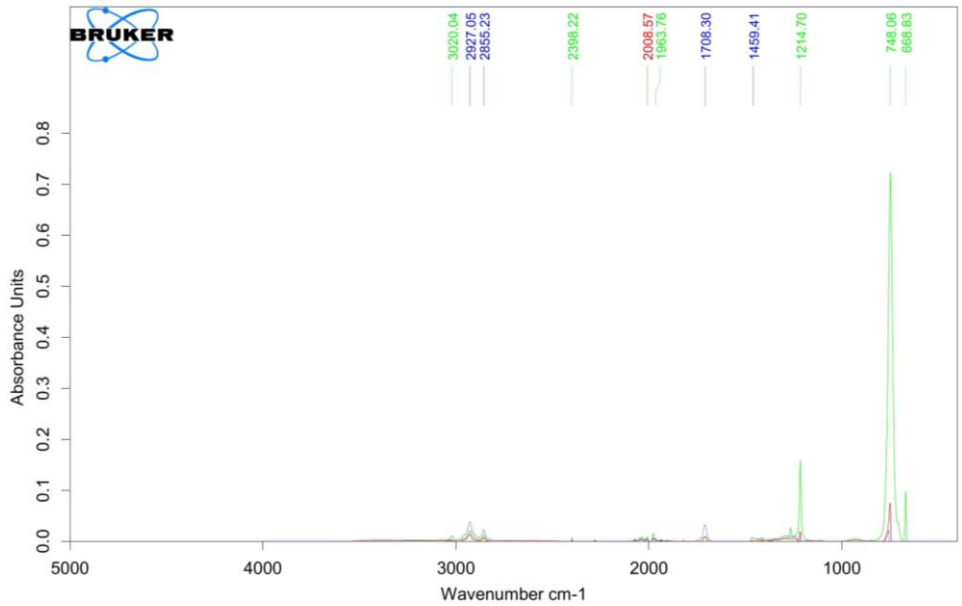

Figure 14:FTIR spectra of Pt/C catalyzed reaction product (Temp=270 ^{0}C, 16% catalyst loading, reaction in water, reaction time=> light green=1h, blue=2h, and red=3h).

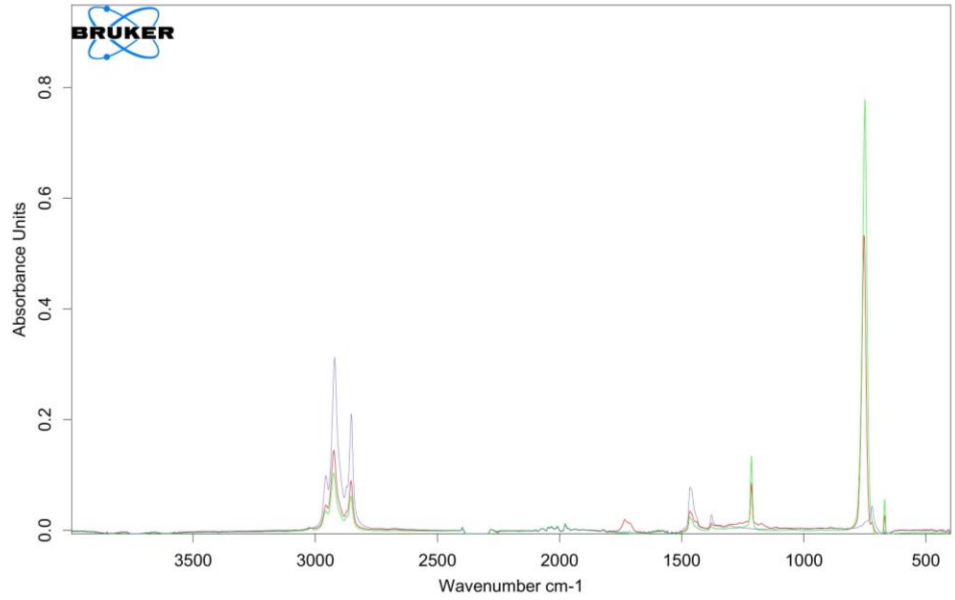

Figure 15: FTIR spectra of Pt/C catalyzed pyrolytic products at 270 ^{0}C and different catalyst loading (red=8wt%, light green=12wt%, and blue=16wt%)

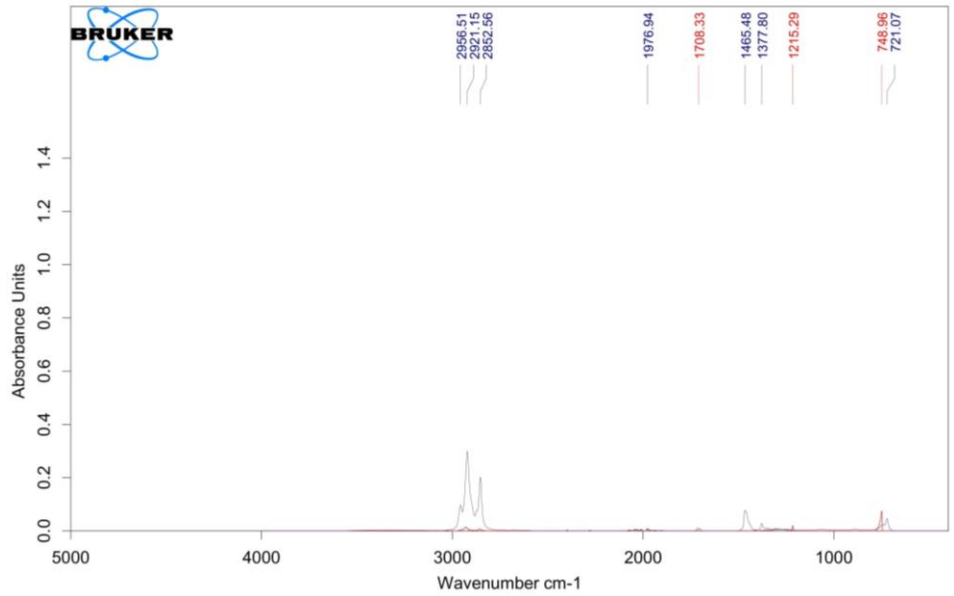

Figure 16: FTIR spectra of Pt/C catalyzed reaction product from catalytic pyrolysis and reaction in water at 270 ^{0}C and 3h (red= reaction in water and blue= pyrolysis)

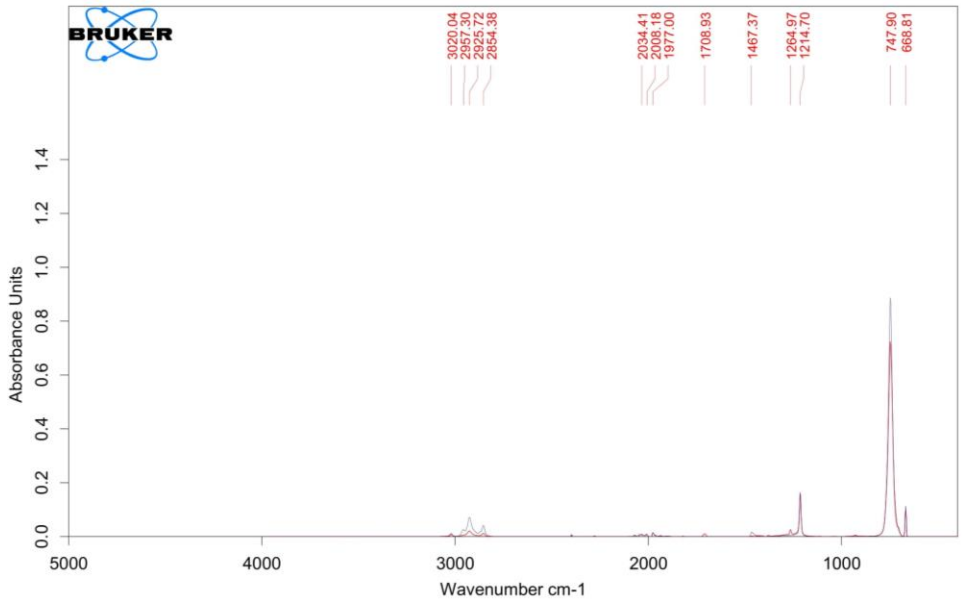

Figure 17: FTIR spectra of Pt/C catalyzed reaction product from catalytic pyrolysis and reaction in water at 270 ^{0}C and 1h (red= reaction in water and blue= pyrolysis)

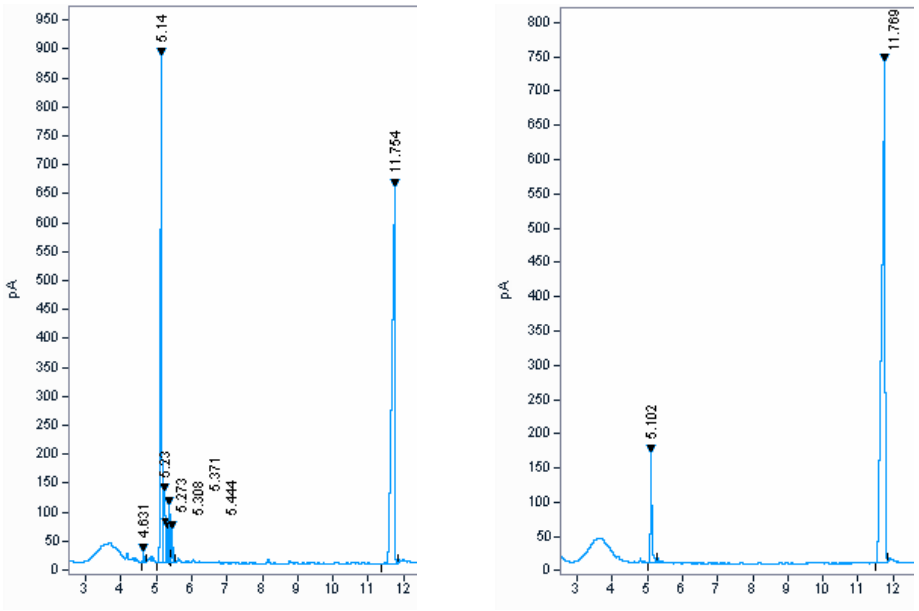

a *b*

*Figure 18: GC-FID chromatogram of **a.** products from Ni/SiAl catalyzed pyrolytic reaction **b.** products from $CoMo/Al_2O_3$ catalyzed pyrolytic reaction (Temp=270 ^{0}C, Time=2h, catalyst loading=16wt%)*

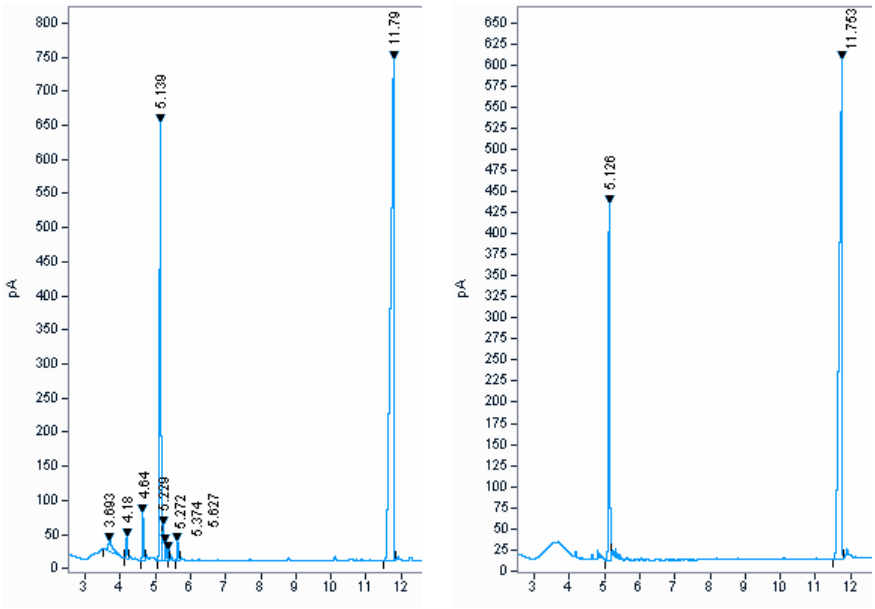

a *b*

*Figure 19: GC-FID chromatogram of **a.** products from Ni/SiAl catalyzed pyrolytic reaction **b.** products from $CoMo/Al_2O_3$ catalyzed pyrolytic reaction (Temp=270 ^{0}C, Time=4h, catalyst loading=16wt%)*

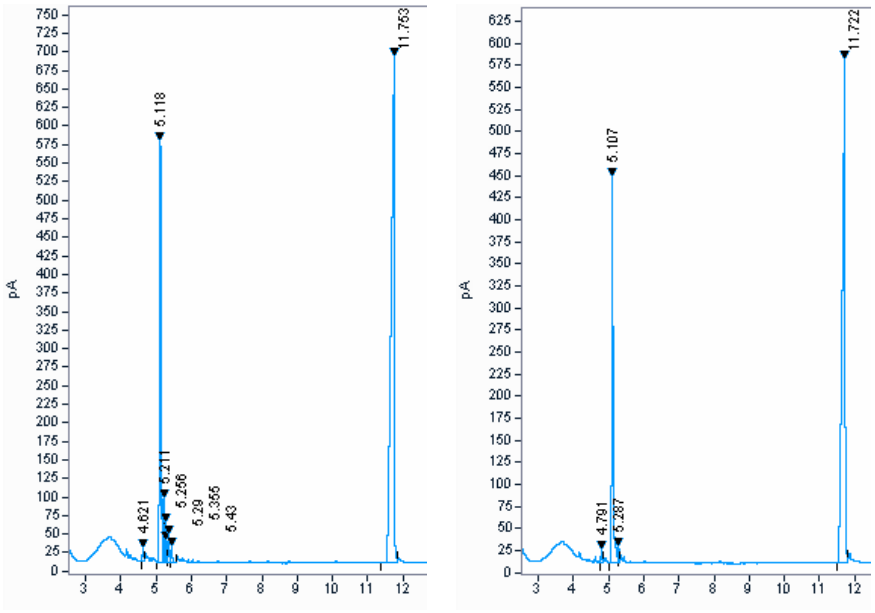

a ***b***

*Figure 20: GC-FID chromatogram of **a.** products from Ni/SiAl catalyzed pyrolytic reaction **b.** products from CoMo/Al_2O_3 catalyzed pyrolytic reaction (Temp=270 ^{0}C, Time=4h (the duplicates to Figure 19), catalyst loading=16wt%)*

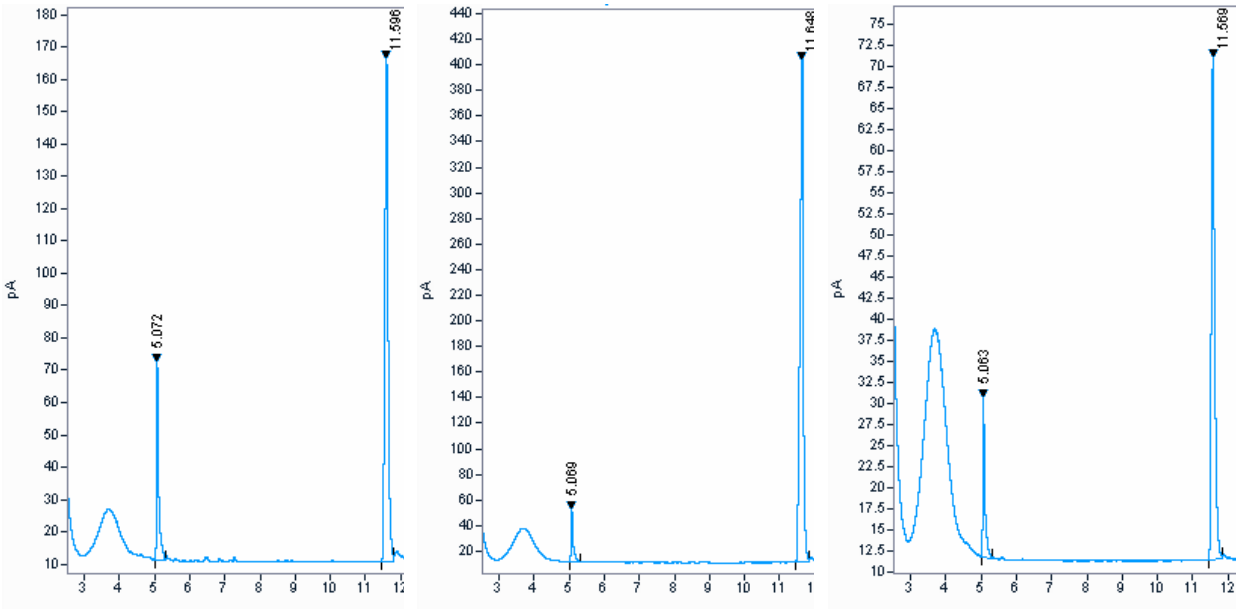

a ***b*** ***c***

*Figure 21: GC-FID of products from Pt/C catalyzed reaction in water at 270 ^{0}C, 16wt% catalyst loading, and different reaction times (**a**=1h, **b**=2h, and **c**=3h)*

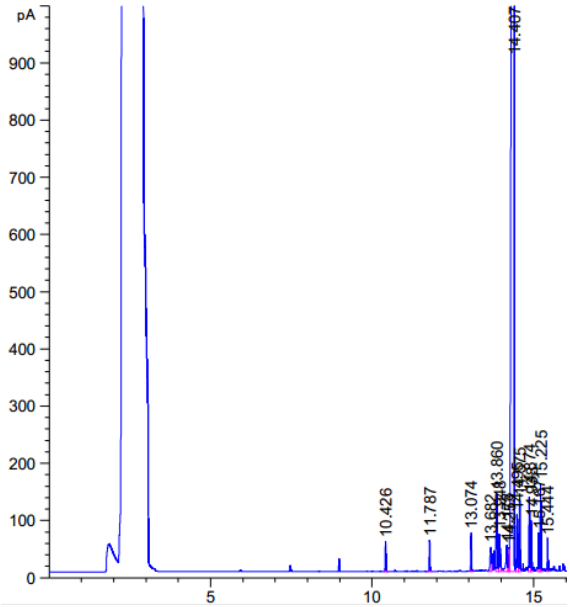

Figure 22: GC-FID chromatogram of liquid product of Pt/C catalyzed pyrolytic reaction at 270 ^{0}C temperature, 2h reaction time, and 12wt% catalyst loading

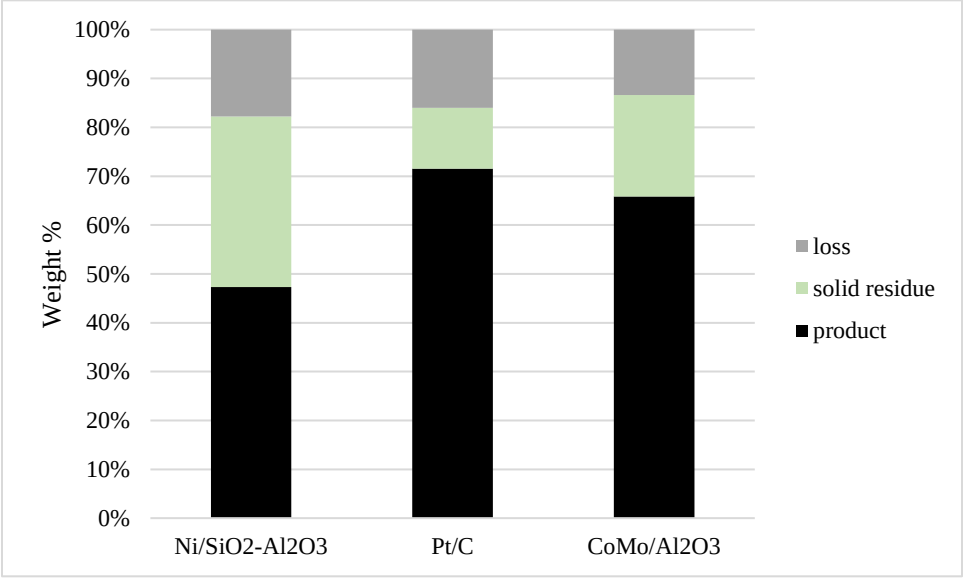

Figure 23: Comparison of mass balance between Pt/C, Ni/ SiAl and CoMo/Al2O3 catalyzed reactions (Temp= 270 ^{0}C and Time=2h)

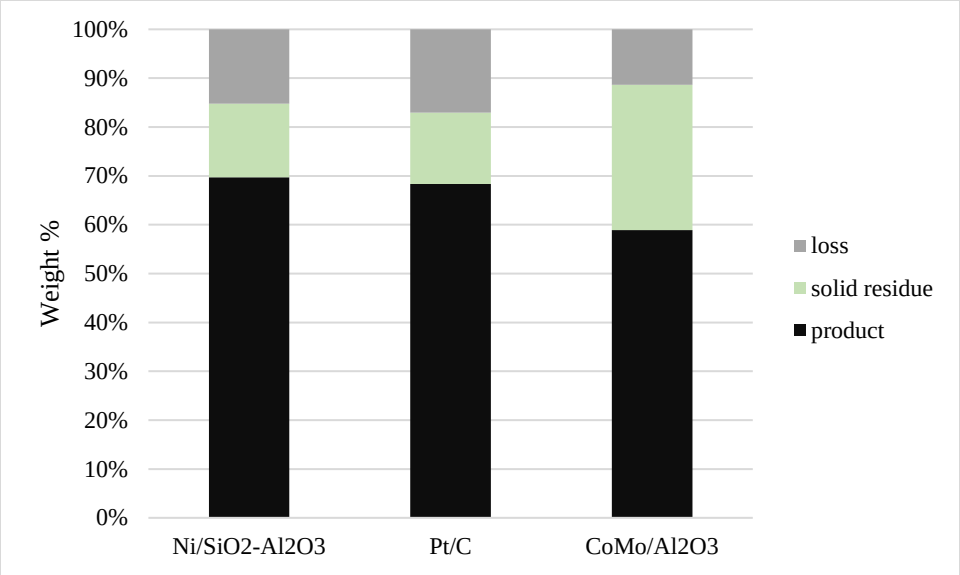

Figure 24: Comparison of mass balance between Pt/C, Ni/ SiAl and CoMo/Al_2O_3 catalyzed reactions (Temp= 270 ^{0}C and Time=4h)

Table 1: Review for catalyst screening

Feedstock	Reaction conditions	Remarks	Ref.
macauba almond oil	5 %Pd/C, 300 ^{0}C, 10 bars H_2, 700 rpm, 5 h, 20:1 (oil to catal. (ml:g)), batch (parr reactor 4348)	85% alkanes	(Silva et al. 2016)
Phoenix Dactylifera kernel	Pd/C, 300 ^{0}C, 10 bars H_2, 500 rpm, 5h, 20:1 (oil to catal. (ml:g))	72.0% diesel and 30.4% jet fuel	(Jamil et al. 2017)
palm kernel oil (palmist oil)	Pd/C, 300 ^{0}C, 10 bars H_2, 600 rpm, 5h, 20:1 (oil to catal. (ml:g)), batch (parr reactor 4348), ,	75% jet fuel yield, 96% conversion, 87% alkanes	(De Sousa, Cardoso, and Pasa 2016)
water soluble fraction of bio-oil	Ru/C, 125 ^{0}C, continous (Packed bed)	Mainly ethylene and propylene glycols and sorbitol	(Sanna, Vispute, and Huber 2015)
water soluble fraction of bio-oil	Pt/C, 250 ^{0}C, continous (Packe bed)	-	(Sanna, Vispute, and Huber 2015)
sunflower, camelina, palm and castor oil	Pt/Al_2O_3/SAPO-11, 370 ^{0}C, 30 bars H_2, benchscale trickle-bed reactor	-	(Rabaev et al. 2015)
soybean oil	Pt/Al_2O_3/SAPO-12, 370-385 ^{0}C, 30 bars H_2, 1%, trickel bed reactor	-	(Rabaev et al. 2015)
n-16 and n-7 alkane	Pt/$SiO_2Al_2O_3$/AlSBA-15 , 320-370 ^{0}C, 50 bars H_2	-	(Jaroszewska et al. 2014)
n-16 and n-7 alkane	PtMo/$SiO_2Al_2O_3$/AlSBA-16, 320-371 ^{0}C, 50 bars H_2	-	(Jaroszewska et al. 2014)
waste fat and oil	(5wt%) Pd/γ-Al_2O_3, 325 ^{0}C, 20 bars H_2, 900 rpm, 1h,2h,5h,20h	-	(Madsen et al. 2011)
waste fat and oil	(5wt%) Ni/γ-Al_2O_3, 325 ^{0}C, 20 bars H_2, 900 rpm, 1,2,5,20h	-	(Madsen et al. 2011)
Fast Pyrolysis oil from beechwood	(5wt%) Ru/C, 250 & 350 ^{0}C, 100 & 200 bars H_2, 1300 rpm, 4h, 5wt% of oil, Batch autoclave	-	(Wildschut et al. 2009)
Fast Pyrolysis oil from beechwood	(5wt%) Ru/TiO_2, 251 & 350, 101 & 200, 1300, 4h, 5wt% of oil, Batch autoclave,	-	(Wildschut et al. 2009)

Fast Pyrolysis oil from beechwood	(5wt%) Ru/Al_2O_3, 252 & 350 ^0C, 102 & 200 bars H_2, 1300 rpm, 4h, 5wt% of oil, Batch autoclave	-	(Wildschut et al. 2009)
Fast Pyrolysis oil from beechwood	(5wt%) Pt/C, 253 & 350 ^0C, 103 & 200 bars H_2, 1300 rpm, 4h, 5wt% of oil, Batch autoclave,	-	(Wildschut et al. 2009)
Fast Pyrolysis oil from beechwood	(5wt%) Pd/C, 254 & 350 ^0C, 104 & 200 bars H_2, 1300 rpm, 4h, 5wt% of oil, Batch autoclave	-	(Wildschut et al. 2009)
soybean oil	NiMo/γ-Al_2O_3, 400 ^0C,20, bars H_2 1h, 4.4wt% of oil, Batch reactor,	92.9% conversion, ~10% selectivity, mainly C17 and C15 alkanes	(Veriansyah et al. 2012)
soybean oil	Pd/γ-Al_2O_3, 400 ^0C, 20 bars H_2, 1h, 4.4wt% of oil, Batch reactor	91.9% conversion, ~5% selectivity, mainly C17 and C15 alkanes	(Veriansyah et al. 2012)
soybean oil	sulfided CoMo, γ-Al_2O_3, 400 ^0C, 29 bars H_2, 1h, 4.4wt% of oil, Batch reactor	78.9% conversion, ~15% selectivity	(Veriansyah et al. 2012)
soybean oil	Ni/SiO_2-Al_2O_3, 400 ^0C, 20 bars H_2, 1h, 4.4wt% of oil, Batch reactor,	60.8% conversion, ~15% selectivity, mainly C17 and C15 alkanes	(Veriansyah et al. 2012)
soybean oil	Pt/γ-Al_2O_3, 400 ^0C, 20 bars H_2, 1h, 4.4wt% of oil, Batch reactor	50.8% conversion, ~10% selectivity	(Veriansyah et al. 2012)
soybean oil	Ru/γ-Al_2O_3, 400 ^0C, 20 bars H_2, 1h, 4.4wt% of oil, Batch reactor	39.7% conversion, ~15% selectivity	(Veriansyah et al. 2012)
palm oil	Co/γ-Al_2O_3, 330 ^0C, 50 bars H_2, trickel bed reactor	0% jet fuel yield	(Srifa et al. 2015)
palm oil	Ni/γ-Al_2O_3, 330 ^0C, 50 bars H_2, trickel bed reactor	0% jet fuel yield	(Srifa et al. 2015)
palm oil	Pd/γ-Al_2O_3, 330 ^0C, 50 bars H_2, trickel bed reactor	0% jet fuel yield	(Srifa et al. 2015)
palm oil	Pt/γ-Al_2O_3, 330 ^0C, 50 bars H_2, trickel bed reactor	0% jet fuel yield	(Srifa et al. 2015)
microalgae pyrolytic bio-oil	Pd/C, 130-250 ^0C, 41-83 bars H_2, 400, 4h, 5% of oil, Batch reactor	-	(Nam et al. 2017)
Technical grade coconut oil	sulfided NiMo/Al_2O_3, 280-380 ^0C, 30 bars H_2,	50-60% jet fuel yield	(Eller, Varga, and Hancsók 2016)
microalgal	NiMoW/ γ-Al_2O_3, NiCoMo/ γ-Al_2O_3, CoMoW/ γ-Al_2O_3, CoNiMoW/γ-Al_2O_3, 400 ^0C, 170, 1 &4h, 25wt% of oil, mini-batch reactor	Mainly C16-C22 alkanes	(D. Xu et al. 2019)
soybean oil	Ni_2P, silica or HY, Bench scale trickel bed reactor	-	(Zarchin et al. 2015)
Pretreated algal oil	Ru/C+Rh/γ-Al_2O_3, 400 ^0C, 240 bars H_2, 4h, 10wt%, Autoclave reactor	-	(Y. Xu, Duan, and Wang 2015)
Pretreated algal oil	Ru/C+Mo_2C, 400 ^0C, 240 bars H_2, 4h, 10wt%, Autoclave reactor	-	(Y. Xu, Duan, and Wang 2015)
Pretreated algal oil	Ru/C+Pt/γ-Al_2O_3, 400 ^0C, 240 bars H_2, 4h, 10wt%, Autoclave reactor	-	(Y. Xu, Duan, and Wang 2015)
Pretreated algal oil	Ru/C+Pt/C, 400 ^0C, 240 bars H_2, 4h, 10wt%, Autoclave reactor	-	(Y. Xu, Duan, and Wang 2015)
microalgae slurry	CoMo, 349 & 405 ^0C, 206 bars H_2, 2h, stirred reactor	25% gasoline, 50% diesel and 25% heavy fuel oil fractions	(Biller et al. 2015)
microalgae slurry	NiMo,350 & 405 ^0C, 66 bars H_2, 2h, stirred reactor,	25% gasoline, 50% diesel and 25% heavy fuel oil fractions	(Biller et al. 2015)
microalgal oil	Ni/C, 300 & 350 ^0C, 500 rpm, 10h, 20wt%, Parr reactor	Mainly in diesel range	(Shakya et al. 2018)
microalgal oil	ZSM-5, 301 & 350 ^0C, 500 rpm, 10h, 20wt%, Parr reactor	Mainly in diesel range	(Shakya et al. 2018)

microalgal oil	Ni/ZSM-5, 302 & 350 ^{0}C, 500 rpm, 10h, 20wt%, Parr reactor	Mainly in diesel range	(Shakya et al. 2018)
microalgal oil	Ru/C, 303 & 350 ^{0}C, 500 rpm, 10h, 20wt%, Parr reactor	Mainly in diesel range	(Shakya et al. 2018)
microalgal oil	Pt/C, 304 & 350 ^{0}C, 500 rpm, 10h, 20wt%, Parr reactor	Mainly in diesel range	(Shakya et al. 2018)
Methyl stearate	Pt/C, 330 &, no H_2, 370 ^{0}C, micro-batch reactor	5%, Conversion, 90% selectivity, Heptadecane	(Fu et al. 2015)
Ethyl stearate	Pt/C, 331 & 370 ^{0}C, no H_2, micro-batch reactor	<80% Conversion, <95% selectivity, alkanes	(Fu et al. 2015)
Stearic acid	Pt/C, 331 & 370 ^{0}C, no H_2, micro-batch reactor	<100% Conversion, <95% selectivity, alkanes	(Fu et al. 2015)
Tristearin	Pt/C, 331 & 370 ^{0}C, no H_2, micro-batch reactor,	<80% Conversion, <90% selectivity, alkanes	(Fu et al. 2015)
Methyl Laurate	Pt/C, 331 & 370 ^{0}C, no H_2, micro-batch reactor	, <50% Conversion, <80% selectivity, alkanes	(Fu et al. 2015)
Methyl eicosanoate	Pt/C, 331 & 370 ^{0}C, no H_2, micro-batch reactor,	<85% Conversion, <100% selectivity, alkanes	(Fu et al. 2015)
Chlorella pyrenoidosa	Pt/γ-Al_2O_3, 400 ^{0}C, 60 bar H_2, 1h, Autoclave reactor		(Duan et al. 2013)
palm oil	Ni/Mesoporous zeolite, 375-475 ^{0}C, 15-25 bar H_2, continuous-flow fixed-bed reactor	~80% selectivity, C8-C16	(Panarmasar, Hinchiranan, and Kuchonthara 2021)
Non-edible veg. oil	Ni/Biochar, 400 ^{0}C, 600 rpm, 1.4wt%, Parr 4598 bench top reactor	-	(Roy et al. 2022)
Non-edible veg. oil	Co/ Biochar, 400 ^{0}C, 600 rpm, 1.4wt%, Parr 4598 bench top reactor	-	(Roy et al. 2022)
Oleic acid	Ru/C/TiO_2, 260 ^{0}C, ~28 bar H_2, 700, Parr series reactors,	<35% jet fuel yield	(Jia et al. 2021)
palm oil	$NiMoS_2$/γ-Al_2O_3, 270-420 ^{0}C, 18-80 bar H_2, continuous-flow fixed-bed reactor	-	(Srifa et al. 2014)
Oleic acid	Ni/ZSM-5, 250 ^{0}C, 10 bar H_2, 2h, fixed-bed flow reactor	51.4% selectivity, Aviation fuel range alkanes	(Feng, Niu, et al. 2020)
Oleic acid	Ni/ γ-Al_2O_3, 340 ^{0}C,	100% conversion, <37.1% selectivity, mainly C16-C18 hydrocarbons	(Feng, Shang, et al. 2020)
microalgal oil (Chlorella)	Al-SBA-15, 300 ^{0}C, 1h, 10wt%, Autoclave micro-reactor,	55.8% jet fuel yield, Hydrocarbons (most aromatic)	(J. Li et al. 2018)
microalgal oil (Chlorella)	CuO/Al-SBA-15, 300 ^{0}C, 1h, 10wt%, Autoclave micro-reactor, no H_2	magnificent selectivity to aliphatic HC& High deoxygenation capability	(J. Li et al. 2018)
microalgal oil (Chlorella)	ZuO/Al-SBA-15, 300 ^{0}C, 1h, 10wt%, Autoclave micro-reactor, no H_2	Magnificent selectivity to aliphatic HC	(J. Li et al. 2018)
microalgal oil (Chlorella)	CuO-ZuO/Al-SBA-15, 300 ^{0}C, no H2, 1h, 10wt%, Autoclave micro-reactor,	65.7% jet fuel yield, magnificent selectivity to aliphatic HC	(J. Li et al. 2018)
Methyl palmitate	Al-SBA-15, CuO/Al-SBA-15, Zu/Al-SBA-15, CuZuO/Al-SBA-15 340 & 350 ^{0}C, 1h, 10wt%, Autoclave micro-reactor, no H_2	30-60% conversion, C12-C15 Alkanes 75.9% selectivity using Al-SBA-15 and 79.6% selectivity using ZuO/Al-SBA-15	(J. Li et al. 2018)
Algal bio-oil	(5%) Pt/C, 400 ^{0}C, 34 bars H_2, 4h, 25wt%, SS bomb reactor,		(Duan and Savage 2011)
Palmitic acid	(5%) Pt/C, <374 & 380 ^{0}C, mini-batch reactor, no H_2,	75 jet fuel yield, ~90% selectivity, mainly pentadecane	(Jang et al. 2010)

Palmitic acid	(5%) Pd/C, <374 & 381 ^{0}C, mini-batch reactor, no H_2	~50% yield, pentadecane	(Jang et al. 2010)
microalgal oil (Botryococcus braunii)	Unsupported CoMoS, 360 ^{0}C, ~90 bars H_2,1000 rpm, 8h, 0.6wt%, Batch reactor	Mainly hydrocarbons	(Ren et al. 2018)
soybean oil	$NbOPO_4$, No Support, 350 ^{0}C, 10 bar N_2 500 rpm, 5h, 15wt%, Parr 4348, bar H_2,	76-90% yield jet fuel hydrocarbons, 58% selectivity	(Scaldaferri and Pasa 2019)
Stearic acid	Pd/ Beta zeolite, 270-330 ^{0}C, bar H_2, 15 bar N_2**,** 300 rpm, 1&3h, 10-25 wt%, Batch reactor	100% conversion, 69.3% of the liquid is jet fuel	(Choi et al. 2015)
soybean oil	Pd/Beta zeolite, 270-331 ^{0}C, no H_2, 15 bar N_2**,** 300 rpm, 1&4h, 10-25 wt%, Batch reactor	100% conversion,	(Choi et al. 2015)
Palm fatty acid distillate	Pd/Beta zeolite, 270-332 ^{0}C, no H_2, 15 bar N_2**,** 300 rpm, 1&5h, 10-25 wt%, Batch reactor	100% conversion,	(Choi et al. 2015)
Oleic acid	Pt/C, 350 ^{0}C, 1.33h, 20wt%, Micro-Batch reactor,	100% conversion, mainly heptadecane	(Tian et al. 2016)
Palmitic acid	Ni, 300 ^{0}C, no H2, 8h, 2mmol, Tubular reactor,	91% selectivity, 60% pentadecane,	(Zhong et al. 2019)
Palmitic acid	Co, 300 ^{0}C, no H_2, 8h, 2mmol, Tubular reactor,	48% pentadecane	(Zhong et al. 2019)
Oleic acid	Activated Carbon, 400 ^{0}C, no H_2, 2h, Tubular reactor	89% to heptadecane, mainly heptadecane	(Hossain, Chowdhury, Jhawar, Xu, and Charpentier 2018)
Jatropha oil	Pd/C, no H_2, 300 ^{0}C, 4h, 10wt%, Batch reactor	Mainly C15 and C17 HC	(Hwang et al. 2016)
Oleic acid	Ni-Pt, 350 ^{0}C, no H_2 20wt%, micro-batch reactor,	90 % heptadecane	(Chen et al. 2020)
Palmitic acid	Ni/ZrO_2, 300 ^{0}C, no H_2, 6h, 100wt%, mini-batch reactor,	~39 paraffin, 64.2, Mainly C8-C15 HC	(Miao et al. 2016)
Fast Pyrolysis oil from beechwood	NiMo/Al_2O_3, 250 & 350 ^{0}C, 100 & 200 bar H_2, 1300 rpm, 4h, 5wt% of oil, Batch autoclave	-	(Wildschut et al. 2009)
Fast Pyrolysis oil from beechwood	CoMo/Al_2O_3, 250 & 350 ^{0}C, 100 & 200 bar H_2, 1300 rpm, 4h, 5wt% of oil, Batch autoclave	-	(Wildschut et al. 2009)